

University of Alberta

Sorption of Cyclohexane on Oil Sands Tailings

by

Lisa Vagi

A thesis submitted to the Faculty of Graduate Studies and Research
in partial fulfillment of the requirements for the degree of

Master of Science

in

Chemical Engineering

Department of Chemical and Materials Engineering

©Lisa Vagi

Fall 2012

Edmonton, Alberta

Permission is hereby granted to the University of Alberta Libraries to reproduce single copies of this thesis and to lend or sell such copies for private, scholarly or scientific research purposes only. Where the thesis is converted to, or otherwise made available in digital form, the University of Alberta will advise potential users of the thesis of these terms.

The author reserves all other publication and other rights in association with the copyright in the thesis and, except as herein before provided, neither the thesis nor any substantial portion thereof may be printed or otherwise reproduced in any material form whatsoever without the author's prior written permission.

Abstract

The use of solvents for extraction of bitumen is attractive because no wet tailings are produced. Studies have already shown that hydrocarbon solvents can achieve the same level of bitumen recovery as the current aqueous extraction method. However, the recovery of solvent must be very efficient to avoid environmental impact and to make the process economic. In order to scale up solvent extraction processes, the adsorption and desorption interactions with mineral surfaces must be quantified. In this study, cyclohexane adsorption and desorption behaviour on clay is characterized by isotherms performed at constant pressure for various temperatures from 20 to 40°C, partial pressures of cyclohexane in nitrogen gas up to 10 kPa, and sample sizes from 50 mg to 2000 mg. These isotherms were classified; the monolayer was calculated, the kinetic behaviour was measured, and the enthalpies of adsorption and desorption were found and compared to the literature value. Only one literature value could be found for comparison.

The isotherm for cyclohexane on clay was classified as a Type II isotherm according to BDDT classification. The BET monolayer coverage varied with temperature. For the range of 20°C to 40°C, the average BET monolayer coverage was calculated to be 0.056 mmol/g for a 50 mg sample. The BET monolayer coverage was calculated to be 0.081 mmol/g for a 2000 mg sample of clay at 30°C, which is comparable to the 0.083 mmol/g monolayer coverage of a sample of pure kaolinite of the same size at the same temperature. Increasing temperature resulted in decreasing adsorbed amount of cyclohexane. There was minimal effect on adsorbed amount when the sample size was changed, as long as it was sampled correctly. The average enthalpy of adsorption and desorption was calculated to be about 40 kJ/mol which is similar to the literature value for cyclohexane on kaolinite. Increasing temperature tended to result in increasing kinetic rate constants while increasing sample size decreased kinetic rate constants. Increasing sample size resulted in decreasing mean kinetic rate constants in general.

Acknowledgements

I would like to thank my supervisor, Murray Gray for his expertise, advice, support, and guidance. Also, I would like to thank Xiaoli Tan for his assistance and training with the IGA and Hossein Nikhakhtari, Phillip Choi, and Qi Liu for their advice and input. I'd like to thank my friends and family for support and encouragement. I am grateful for the financial support provided by the Centre for Oil Sands Innovation (COSI) at the University of Alberta.

Table of Contents

1.0 Introduction.....	1
1.1 Selection of Solvent	1
1.2 Objectives	3
2.0 Literature Review.....	4
2.1 Past Studies of Non-Aqueous Extraction.....	4
2.1.1 Solvent and Solvent Mixtures	4
2.1.2 Solvent Extraction Spherical Agglomeration Process	4
2.1.3 Supercritical Extraction Processes	5
2.2 Non-Aqueous Extraction Tailings and Soil Remediation.....	5
2.3 Adsorption and Desorption Studies	5
3.0 Theory	7
3.1 Isotherm Classification	7
3.2 BET Theory	8
3.3 Linear Driving Force Model	10
3.4 Van't Hoff Isochore	11
4.0 Experimental Methods	13
4.1 Materials	13
4.2 Aqueous Clay Extraction Method.....	13
4.3 Intelligent Gravimetric Analyzer	14
4.4 Isotherm Experimental Method	14
5.0 Results and Discussion	17
5.1 Repeatability of Isotherms	17
5.2 Classification of Isotherm.....	18
5.3 Temperature Dependence of Isotherm.....	19

5.3.1 BET Monolayer Coverage	21
5.3.2 Enthalpy of Adsorption.....	22
5.4 Kinetics of Adsorption and Desorption	23
5.4.1 Repeatability of Adsorption and Desorption	23
5.4.2 The Effect of Temperature on Sorption Kinetics.....	24
5.5 Effect of Sample Size and Sampling	29
5.5.1 Equilibrium Sorption	29
5.5.2 Sorption Kinetics	30
6.0 Conclusions.....	34
References.....	35

List of Tables

Table 1. Solvents used for solvent extraction of oil sands and their performance based on bitumen recovery, fines in recovered bitumen, and residual solvent in the tailings [5]. .	2
Table 2. List of chemicals used.....	13
Table 3. Isothermal adsorption and desorption solvent concentration steps.	16
Table 4. Monolayer coverage for toluene and cyclohexane on centrifuged solids, and 2000 mg samples of kaolinite and clay at 30°C.....	21

List of Figures

Figure 1. A sketch of the isotherm classification proposed by Brunauer, Deming, Deming, and Teller (BDDT) in 1940.	8
Figure 2. BET model of cyclohexane adsorption onto a 50 mg sample of clay at 25°C.....	10
Figure 3. The average of three runs with error bars for a sorption isotherm of cyclohexane on a 2 g clay sample at 20°C.	17
Figure 4. Sorption isotherm for cyclohexane on a 50 mg clay sample at 20°C.....	18
Figure 5. Sorption isotherms at three temperatures for cyclohexane on a 50 mg sample of clay.	20
Figure 6. Classically plotted sorption isotherms at three temperatures for cyclohexane on a 50 mg sample of clay.	20
Figure 7. BET monolayer for cyclohexane on clay at several temperatures for a 50mg sample.	21
Figure 8. Absolute value of enthalpies of sorption for adsorption and desorption of cyclohexane on clay.	23
Figure 9. Sorption kinetics for three runs of cyclohexane on a 2 g clay sample at 20°C.	24
Figure 10. Adsorption rate constants for cyclohexane on a 50 mg clay sample at various temperatures.	26
Figure 11. Desorption rate constants for cyclohexane on a 50 mg clay sample at various temperatures.	26
Figure 12. Adsorption rate constants versus amount of cyclohexane adsorbed on a 50 mg clay sample at various temperatures.	27
Figure 13. Desorption rate constants versus amount of cyclohexane adsorbed on a 50 mg clay sample at various temperatures.	27
Figure 14. Three dimensional graph of rate constant versus partial pressure versus temperature of cyclohexane adsorbed on a 50 mg sample of clay.....	28
Figure 15. Three dimensional graph of amount adsorbed versus partial pressure versus temperature of cyclohexane adsorbed on a 50 mg sample of clay.	28
Figure 16. Three dimensional graph of rate constant versus partial pressure versus amount adsorbed at various temperatures for cyclohexane adsorbed on a 50 mg sample of clay.	29
Figure 17. The effect of sample size on equilibrium sorption of cyclohexane on clay at 30°C.	30
Figure 18. Adsorption rate constants for cyclohexane on clay at 30°C for various sample sizes.	31
Figure 19. Desorption rate constants for cyclohexane on clay at 30°C for various sample sizes.	31

Figure 20. Adsorption rate constants versus amount of cyclohexane adsorbed on clay at 30°C for various sample sizes.	32
Figure 21. Desorption rate constants versus amount of cyclohexane adsorbed on clay at 30°C for various sample sizes.	32
Figure 22. Mean rate constants versus sample size for adsorption and desorption of cyclohexane on clay at 30°C.	33

List of Symbols

A	Slope of the BET linear plot
$\bar{C}(t)$	Average adsorbate concentration, mol/L
$\bar{C}^*(t)$	Average adsorbate concentration at equilibrium, mol/L
c	BET constant
ΔH	Differential molar enthalpy of adsorption, kJ/mol
H_1	Enthalpy of adsorption, kJ/mol
H_L	Enthalpy of condensation, kJ/mol
I	Intercept of the BET linear plot
K	Equilibrium constant, kPa g/ mmol
k	Kinetic rate constant, s ⁻¹
M_e	Mass uptake, g at equilibrium
M_t	Mass uptake, g at time t
n	Amount adsorbed, moles
n_a	Amount adsorbed, mmol/g
n_m	BET monolayer, mmol/g
P	Partial pressure, kPa
P_o	Saturation pressure, kPa
q^{st}	Isosteric heat of adsorption
R	Universal gas constant
T	Temperature, °C
t	Time

1.0 Introduction

The Canadian oil sands in northern Alberta are the second largest proven reserve of petroleum in the world, second to Saudi Arabian reserves [1]. The most pressing problem facing the oil sands mining industry in Alberta is the management of wet tailings. Wet tailings comprise mainly sand, fine solids dominated by clays like kaolinite and illite, and residual bitumen [2, 3]. The accumulation of mature fine tailings from aqueous extraction dominates mine planning, delays reclamation, and causes unwanted environmental impact and negative public perception.

Solvent extraction of mined oil sands has been studied since the 1970s and was abandoned due to high solvent losses [4]. The solvent used to extract the bitumen is often more expensive than the bitumen recovered. Therefore, the ability to recycle all of the solvent is very important. Due to concerns about water consumption and the size of wet tailings ponds today, solvent extraction of mined oil sands has resurfaced at the forefront of oil sands research.

In many ways, the process of solvent recovery is similar to soil remediation. Most often, soil remediation simply involves allowing the volatile organic compounds (VOCs) to evaporate naturally from the contaminated soil. This process is slow and often takes years to reach acceptable levels. Soil remediation techniques are often designed to preserve the soil organic materials (SOM), which are analogous in chemical structure to bitumen and asphaltenes in the oil sands. Although solvent recovery processes are not intended to preserve these components, they do involve similar interaction effects between the solvent and the oil sands.

In order for the solvent recovery process to be economically feasible, it must have low energy requirements, acceptable levels of solvent in the clean tailings, near 100% solvent recycle, and take a reasonable amount of time to occur.

1.1 Selection of Solvent

The solvent in this study, cyclohexane, was chosen as a result of previous work by Nikakhtari et al. soon to be published in the Canadian Journal of Chemical Engineering [5]. A number of organic solvents were evaluated based on bitumen recovery, the amount of residual solvent in the extracted oil sands tailings, and the content of fine solids in the extracted bitumen. The extraction experiments were carried out in a multistage batch process at ambient conditions that was

developed by Hooshiar et al. [6]. The multistage batch process included agitation in rotary mixers, settling, and vibration sieving. The work by Nikakhtari et al. found that cyclohexane is the best candidate solvent for bitumen extraction, with 94.4 % bitumen recovery, low residual solvent in extraction tailings, and low fine solids in the recovered bitumen. The following table lists the solvents used and the performance of each solvent and solvent mixture from Nikakhtari et al.

Table 1. Solvents used for solvent extraction of oil sands and their performance based on bitumen recovery, fines in recovered bitumen, and residual solvent in the tailings [5].

Solvent	Bitumen Recovery, %	Fine Solids in the Recovered Bitumen, % of ore extracted	Residual Solvent Concentration in the Tailings, mg/kg of tailings
100% Toluene	96.3 ± 1.1	0.07 ± 0.03	210
70% Toluene/ 30% n-Heptane	94.3 ± 2.3	0.16 ± 0.10	108
50% Toluene/ 50% n-Heptane	95.9*	0.07*	n/a
30% Toluene/ 70% n-Heptane	95.8 ± 2.5	0.63 ± 0.22	93
20% Toluene/ 80% n-Heptane	95.9*	1.37*	n/a
10% Toluene/ 90% n-Heptane	92.6 ± 3.2	2.33 ± 0.64	89
Methyl Cyclohexane	94.9*	0.24*	29
Cyclohexane	94.4 ± 1.7	0.11 ± 0.04	5
10% Toluene/ 90% Cyclohexane	93.2*	0.10*	20
Ethylbenzene	93.8*	0.07*	407
Xylenes	93.4*	0.08*	448
Isoprene	91.4 ± 1.5	0.38 ± 0.09	1
Limonene	53.0*	0.11*	370

*Single data point, no replication was carried out. All other data point are 3 repetitions or more.

1.2 Objectives

Before the solvent recovery process for solvent extraction of oil sands can be modelled, the adsorptive and desorptive behaviour of the solvent on the tailings needs to be characterized. After the solvent recovery process has been modelled, process design, followed by pilot plant testing, can begin and solvent extraction of oil sands could become a feasible alternative to current aqueous bitumen extraction technologies.

The objectives of this investigation are outlined below:

- Characterize sorption behaviour of cyclohexane on clay
- Explore effects of temperature and sample size on:
 - Amount adsorbed
 - Kinetic rate constants
- Compare results with cyclohexane vapour on pure kaolinite and with literature values
- Calculate the enthalpy of adsorption and desorption
- Calculate the monolayer adsorbed amount

The above objectives will be achieved by manipulating temperature, sample size, and solvent concentration while keeping pressure and total flow rate constant. The sample mass and adsorbed amount as a function of time will be recorded.

2.0 Literature Review

Since the 1920s, all commercial operations for surface mined oil sands in Northern Alberta have extracted bitumen using the Clark Hot Water Extraction process or a variation of it [7]. However, extraction of bitumen using organic solvents has also been researched since the 1960s. The following section describes these efforts.

2.1 Past Studies of Non-Aqueous Extraction

2.1.1 Solvent and Solvent Mixtures

Literature on solvent extraction can be found as early as a US patent from 1968 describing the process of solvent extraction of McMurray formation oil sands [8]. The solvents used were referred to as “soluble oils”. These may have been naphtha or other light oils. Another US patent from 1986 uses a solvent mixture of toluene and methyl cyclohexane [9]. Mixtures of toluene and heptane have also been studied for the non aqueous extraction of bitumen from oil sands [6, 10]. These and other appropriate solvents are highly volatile and flammable. Another US patent in 1974 described an apparatus that is completely enclosed to prevent solvent vapour losses [11]. The majority of these solvent extraction processes had a solvent contacting stage followed by solid-liquid separation usually in the form of settling and some had a solvent recovery or recycle unit. Scientific studies are lacking in this technology due to the prevalence and economic feasibility of bitumen extraction using water. Since water was abundant at the time, solvent extraction was abandoned due to solvent losses and the solvent being more expensive than the bitumen being extracted.

2.1.2 Solvent Extraction Spherical Agglomeration Process

In 1988 the Solvent Extraction Spherical Agglomeration (SESA) process was patented and incorporated water as a binding agent in the solvent [12]. The SESA process was developed to reduce the accumulation of sludge in the tailings ponds [13]. The water bridged clay particles together and reduced the organic content of agglomerated clay sand in the tailings substantially, leading to higher bitumen recovery as well. However, uneconomical solvent losses were a problem.

2.1.3 Supercritical Extraction Processes

Supercritical fluid extraction of bitumen from oil sands in Utah was studied with propane as a solvent [14]. The supercritical fluid solvent provided two purposes: to extract the bitumen and also upgrade the bitumen by reducing its asphaltene content. Supercritical carbon dioxide extraction showed bitumen recovery of up to 45 % [14], which is poor compared to the bitumen recovery rates by solvent extraction by Nikakhtari et al. [5]. The low recovery rate by supercritical carbon dioxide extraction is likely due to the low solubility of bitumen in supercritical carbon dioxide making the process uneconomical. As a result, a high recycle ratio of supercritical carbon dioxide is required, meaning that several volumes of supercritical carbon dioxide would be used and recycled for each volume of oil sands processed. Also, it is impractical to operate a continuous process at high pressures that contains sand because sand has been known to cause extreme wear on equipment and equipment seals [15].

2.2 Non-Aqueous Extraction Tailings and Soil Remediation

Vapour extraction of volatile organic compounds in excavated contaminated soil has been studied and developed successfully for commercial use [16]. The research in this area provides a valuable analogy for the desorption of solvent from tailings of non-aqueous oil sands extraction. Kaolinite, a common component of soil, has been found by clay mineralogy analysis to be a major component in the fine solids fraction of Athabasca oil sands and tailings [2]. Fine solids are defined as solids that are less than 45 μm in diameter. Studies on factors affecting soil remediation have shown that increased moisture content on clays aids the displacement of volatile organic compounds [17]. This knowledge can be applied similarly with the competitive adsorption of water with organic solvent on tailings from non aqueous extraction in future studies. Studies have found that sorption kinetics of organic vapours in soil organic matter (SOM) is slow and desorption is difficult [18]. SOM could be analogous to residual bitumen and asphaltenes in oil sand tailings.

2.3 Adsorption and Desorption Studies

The kinetics and thermodynamics of adsorption and desorption of gases onto solids has been studied extensively on kaolinite [17, 19], zeolites [20], and activated carbon [21, 22] for the

purposes of soil remediation, purifying nitrogen, or absorbing contaminants from air. These studies have shown that all three of these solids have a large capacity for adsorption. Although this property is advantageous for use as an absorbent, it shows that kaolinite is the component in the solvent extraction tailings that is of most concern for solvent retention.

The experimental method in this study was influenced greatly by the methods of Fletcher and Thomas [21]. Isotherms were performed at various temperatures in order to obtain the isosteric enthalpies of adsorption using an Intelligent Gravimetric Analyser supplied by Hiden Isochema, the same equipment for this study. However, no previous adsorption isotherm data could be found for the specific case in this study of cyclohexane adsorbed onto kaolinite at ambient temperatures. This has made comparison of data to literature values difficult in this study. Nevertheless, valuable comparisons can still be made.

3.0 Theory

3.1 Isotherm Classification

An adsorption isotherm is a representation of the relationship between the amount of adsorbate adsorbed to the adsorbent at various relative pressures under isothermal conditions. The adsorbate is the material that adsorbs to the substrate known as the adsorbent. Relative pressure is the partial pressure, P , (a form of molar concentration) divided by the saturation pressure, P_o , of a particular gas. Using relative pressure on the x-axis allows for the comparison of adsorption isotherms with different adsorbates. Adsorption isotherms are grouped into five classes proposed by Brunauer, Deming, Deming, and Teller (BDDT) in 1940 [23]. A sketch of these five classes is shown in Figure 1. Type I isotherms are characteristic of microporous adsorbents. Type II isotherms indicate that the solid is non-porous, while Type IV isotherms are characteristic of a mesoporous solid. Type III and V isotherms are characteristic of systems where the adsorbent-adsorbate interaction is unusually weak, and are much less common than isotherms of the other types.

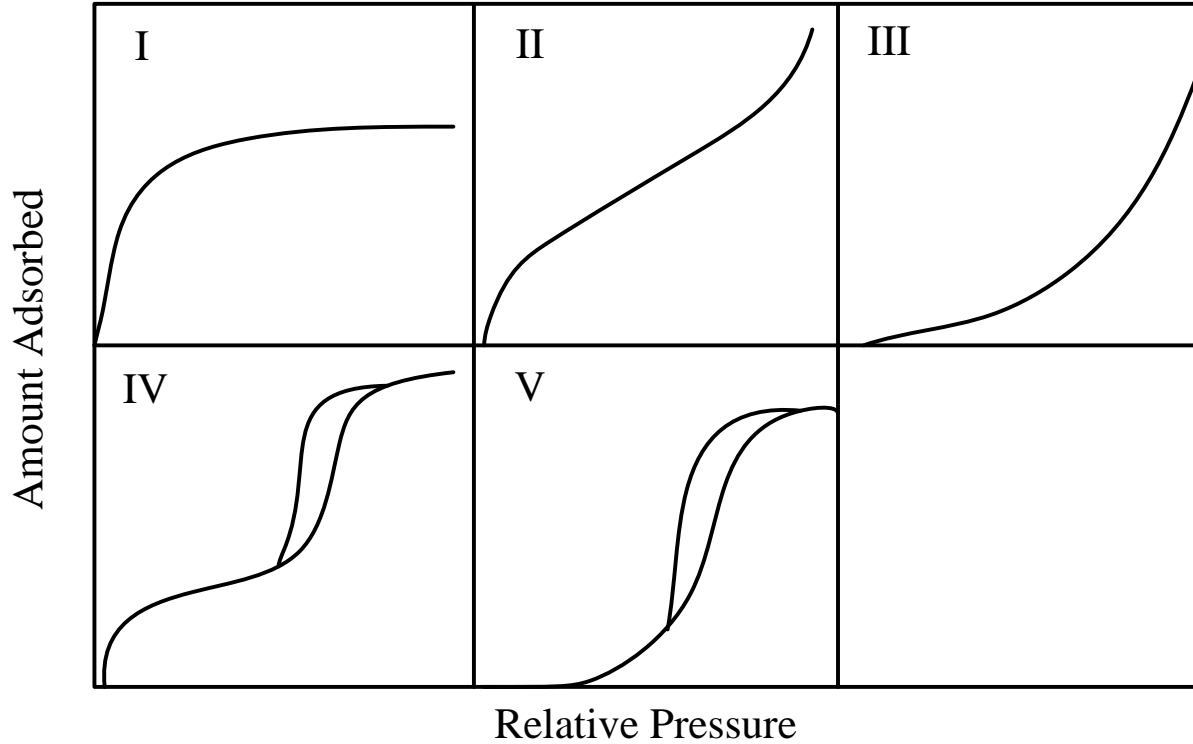


Figure 1. A sketch of the isotherm classification proposed by Brunauer, Deming, Deming, and Teller (BDDT) in 1940.

3.2 BET Theory

The Brunauer, Emmett, and Teller (BET) model has its roots in a kinetic model of the adsorption process by Langmuir [24], in which the surface of the solid is considered to be a series of finite adsorption sites. At equilibrium, the rate at which molecules condense from the gas phase onto the open adsorption sites equals the rate at which molecules evaporate from occupied sites. Brunauer, Emmett and Teller in 1938, built onto Langmuir's theory to include multilayer adsorption to include three simplifying assumptions: (a) that in all layers except the first the enthalpy of adsorption is equal to the molar enthalpy of condensation; (b) that in all layers except the first the evaporation-condensation conditions are identical; (c) that when the partial pressure equals the saturation pressure, the adsorbate condenses into a bulk liquid on the surface of the solid and the number of layers becomes infinite [25, 26].

The following equation shows the BET equation in a form convenient for plotting, in which

$$y = \frac{1}{n[(P_0/P)-1]}, \quad x = \frac{P}{P_0}, \quad \text{the slope} = \frac{c-1}{n_m c}, \quad \text{and the intercept} = \frac{1}{n_m c}$$

$$\frac{1}{n[(P_0/P) - 1]} = \frac{c - 1}{n_m c} \left(\frac{P}{P_0}\right) + \frac{1}{n_m c} \quad (1)$$

$$c = \exp\left(\frac{H_1 - H_L}{RT}\right) \quad (2)$$

$$n_m = \frac{1}{A + I} \quad (3)$$

$$c = 1 + \frac{A}{I} \quad (4)$$

where A is the linear best fit slope of a plot of Equation (1) and I is the intercept. The c constant can be used to determine the enthalpy of sorption, H_1 , if the enthalpy of condensation, H_L , is known. The monolayer is n_m and the molar uptake is n , and relative pressure is P/P_0 .

According to the BET model, the above plot is linear only for relative pressure between 0.05 and 0.35 [26] and this investigation uses data only in this range to calculate the BET monolayer. The adsorption of cyclohexane onto clay is similar to the interaction of cyclohexane adsorbed onto alumina, for which the BET plot is known to be non-linear in many cases and no explanation is offered in the literature [25]. Figure 2 shows the non-linearity of a BET plot from this investigation of cyclohexane adsorption onto a 50 mg sample of clay at 25°C by plotting a linear line of best fit over the data. Although the R^2 value is close to 1 (greater than 0.95), it can be seen clearly that the residuals are not randomly distributed. Therefore, the data is non-linear.

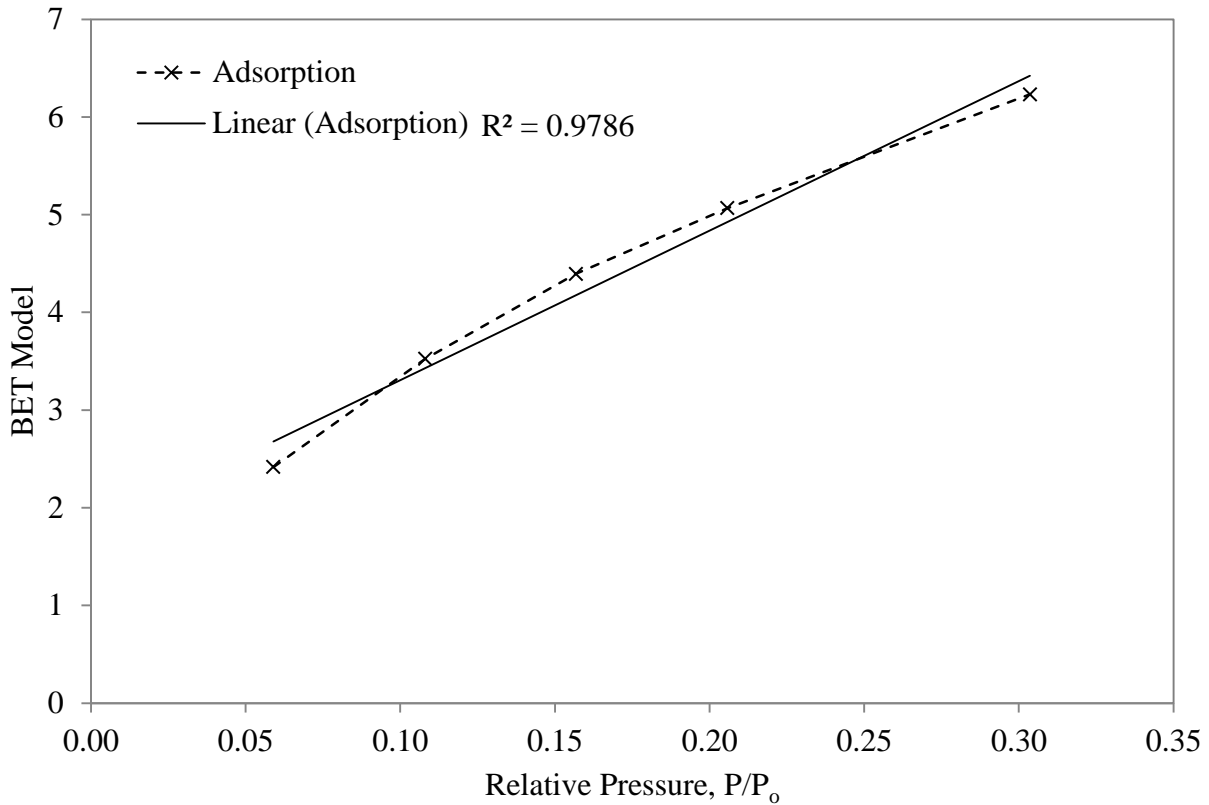


Figure 2. BET model of cyclohexane adsorption onto a 50 mg sample of clay at 25°C.

3.3 Linear Driving Force Model

The Linear Driving Force (LDF) Model was chosen to analyze the kinetics of sorption for this investigation because it is simple, widely used, and provided enough analysis for the purposes of this investigation. It was also conveniently integrated into the IGA software. The LDF model is based on the existence of a barrier resistance at the surface and subsequent diffusion into a spherical particle governed by Fick's law [21]. The substrate in this investigation is not spherical and contains macro and micro pores. The LDF model is a simple one with only two components vapour and solid. In this investigation, there are a number of complex components because the substrate is heterogeneous and is known to contain residual bitumen and asphaltenes. Knowing how the experimental conditions differ from the theory of the model helps to interpret the meaning of the parameters.

The experiments were performed at constant pressure so the following equation applies

$$M_t/M_e = 1 - e^{-k t} \quad (5)$$

where M_t is the mass uptake at time t , M_e is the equilibrium mass uptake, and k is the rate constant. The rate constant can be obtained from the slope of a plot of $\ln(1-M_t/M_e)$ versus time.

The LDF model is based on the principle that the adsorptive force is linearly dependent on the difference between the equilibrium concentration and the current concentration of the gas. This is shown in the following equation which the above equation was derived from

$$\frac{d\bar{C}(t)}{dt} = k[\bar{C}^*(t) - \bar{C}(t)] \quad (6)$$

where $\bar{C}(t)$ is the average adsorbate concentration in moles per unit volume, $\bar{C}^*(t)$ is the equilibrium average adsorbate concentration, and k is the effective LDF mass transfer coefficient or rate constant.

The rate constants were obtained from the mass versus time graphs of each step up or down during an isotherm experiment. The IGA software was used to fit the model equation to approximately 10 minutes of data with residuals less than 50 μg .

3.4 Van't Hoff Isochore

The isosteric enthalpies of adsorption were calculated using the van't Hoff isochore. Isosteric means keeping the amount adsorbed constant and an isochore is the relation between temperature, concentration, and enthalpy at a given adsorbed amount of adsorbate on the adsorbent. At equilibrium, the following equation holds at a given amount adsorbed, n_a

$$\left(\frac{\partial \ln K}{\partial T}\right)_{n_a} = -\frac{\Delta H}{RT^2} \quad (7)$$

where ΔH is the differential molar enthalpy of adsorption and is negative when adsorption occurs, and heat is therefore released. Alternatively, this term is often called the isosteric heat of adsorption (q^{st}) and is given the opposite sign. The equilibrium constant, K , is equal to the partial

pressure of solvent in the carrier gas divided by the amount of adsorbate adsorbed. If multiple isotherms at several temperatures are available, a plot of the natural logarithm of the equilibrium constant, K , versus the reciprocal temperature gives a straight line. The above equation can be also written as

$$\ln K = -\frac{\Delta H}{RT} + \text{constant} \quad (8)$$

This equation represents an adsorption isostere, which is the relation between concentration and temperature for a given amount adsorbed. The molar enthalpy of adsorption can be calculated from the slope of the plot.

4.0 Experimental Methods

4.1 Materials

The oil sands ore sample was provided by Syncrude Canada Ltd. Dean-Stark extraction of the ore sample showed 13.5±1.1% bitumen, 3.0±0.9% water, and 11.2±0.7% fines, which is classified as a rich ore [5]. Solvents used were Certified ACS from Fisher Scientific Canada. A list of chemicals is provided in Table 2.

Table 2. List of chemicals used.

Chemical	Manufacturer	Purity (%) and/or Grade
Cyclohexane	Fischer Scientific	Certified ACS Grade
Toluene	Fischer Scientific	Certified ACS Grade
Nitrogen	PRAXAIR Canada Inc.	N/A
Kaolinite – $\text{Al}_2\text{Si}_2\text{O}_5(\text{OH})_4$	Ward's Natural Science, USA	N/A

4.2 Aqueous Clay Extraction Method

Dean-Stark extraction with toluene on a Soxhlet extractor was used to remove bitumen from approximately 250 grams of oil sands ore. The Soxhlet extracted oil sands were mixed vigorously with water and then allowed to briefly settle (15 to 45 minutes). The liquid was siphoned off and centrifuged for 1 hour. A Model 138 Avanti J-30I centrifuge (Beckman Coulter, Mississauga, ON), with JA-10 rotor, 250 mL Teflon containers was used. The centrifuge was operated at a relative centrifugal force of 4000. The clear liquid was siphoned off and the solids were dried in the vacuum oven at 70°C and 1 atm vacuum over night. The mixing, siphoning, and centrifuging was repeated until enough sample was obtained. The solid sediment was scraped off the containers and ground into a powder to be tested in the Intelligent Gravimetric Analyzer (IGA) for sorption behaviour. This produced approximately 5 grams of solids that appear to be less than 45 µm, which, for the purposes of this study, will be referred to as “clay” although they may contain some non-clay mineral. As well, a comparison with pure

kaolinite fine clay powder will be made. This method was developed from personal previous experience with soil testing as a fast method for isolating clay from a soil mixture.

Aqueous suspension tends to isolate the highly hydrophilic clay particles from the sand matrix. The clay was chosen for investigation because previous studies showed that clays, especially kaolinite, were problematic in solvent losses [19].

4.3 Intelligent Gravimetric Analyzer

The Intelligent Gravimetric Analyzer (IGA), manufactured by Hiden Isochema of Manchester, United Kingdom, is capable of measuring small changes in mass (as small as 0.001 mg) of a sample that is exposed to various conditions. Temperature, pressure, gas flow, and solvent concentration can be controlled and measured precisely by a vapour generator and a desktop computer. The sample is loaded into the sample chamber in a stainless steel mesh bucket.

4.4 Isotherm Experimental Method

Before each adsorption isotherm measurement, the clay sample was pretreated at 110°C and 105 kPa for 8 hours to desorb all water. The sample chamber was heated using an electric heater. Then the sample was cooled to 30°C inside the sample chamber.

Purified nitrogen carrier gas was bubbled through cyclohexane solvent in a vapour generator at a controlled temperature (20°C) before entering the sample chamber at constant temperature and constant 105 kPa pressure that contains a bucket holding a clay sample. To prevent condensation, electric heat tracing was used on the line connecting the vapour generator to the sample chamber. The total gas flow of 100 mL/min was kept constant for all runs. The change in mass of the sample was recorded every three seconds along with temperature, pressure, and flow rate of the carrier gas and solvent-saturated gas. The concentration of cyclohexane in the nitrogen carrier gas was controlled by the computer which operates a manifold that mixes pure nitrogen carrier gas with solvent-saturated nitrogen gas from the vapour generator.

Tests were performed beforehand to determine the minimum time required for the mass change to equilibrate. This was found to be approximately 3 hours. The computer was programmed to change the solvent concentration in 3 hour steps. After each isotherm, the data was checked

visually to ensure equilibrium was achieved at each step. If the mass versus time graph showed a flat region of no mass change before the next step, then equilibrium had been achieved.

Beginning at 0% the concentration of solvent in the carrier gas was stepped at 13 precise intervals up to 95% saturated solvent vapour and then back down to 0%, which were kept consistent for every isotherm and are listed in Table 3. Each isotherm took approximately 5 days including pre-treatment. Due to time constraint, all runs were not repeated and were performed only once. One run at 20°C for a 2 g clay sample was repeated 3 times to ensure repeatability of the results.

At first, the temperatures of the sample chamber and vapour generators were kept equal. This led to some complications at temperatures above 30°C. The solvent reservoir would need to be refilled and the experiment restarted. This led to hysteresis in the isotherms around the point that the isotherm was restarted. Results were difficult to repeat. It is important that the vapour generator temperature be lower than or equal to the sample chamber temperature to prevent condensation. So the vapour generators were kept at 20°C and the sample chamber temperature varied. This produced much more repeatable results. Concerns were raised about the consistency of the sample chamber temperature as gas at a lower temperature from the vapour generators is pumped into the chamber. The total gas flow of 100 mL/min was determined to be very slow with a Reynolds number between 1 and 1.5. This means that the gas has ample time to equilibrate in the sample chamber.

Table 3. Isothermal adsorption and desorption solvent concentration steps.

Adsorption		Desorption	
% Flow of solvent-saturated gas stream	Calculated partial pressure of solvent, kPa	% Flow of solvent-saturated gas stream	Calculated partial pressure of solvent, kPa
0	0.00	95	9.81
5	0.62	90	9.30
10	1.13	85	8.79
15	1.64	80	8.28
20	2.15	70	7.26
30	3.17	60	6.24
40	4.19	50	5.21
50	5.21	40	4.19
60	6.24	30	3.17
70	7.26	20	2.15
80	8.28	15	1.64
85	8.79	10	1.13
90	9.30	5	0.62
95	9.81	0	0.00

5.0 Results and Discussion

The results of this investigation are provided in a logical progression. It begins with an analysis of the repeatability of the experiments, and then is followed by the classification of a typical isotherm. The effect of temperature on sorption isotherm, BET monolayer coverage, and then enthalpy of adsorption is presented. The kinetics of adsorption and desorption are presented along with their repeatability and effect of temperature. Finally, the effect of sample size is presented.

5.1 Repeatability of Isotherms

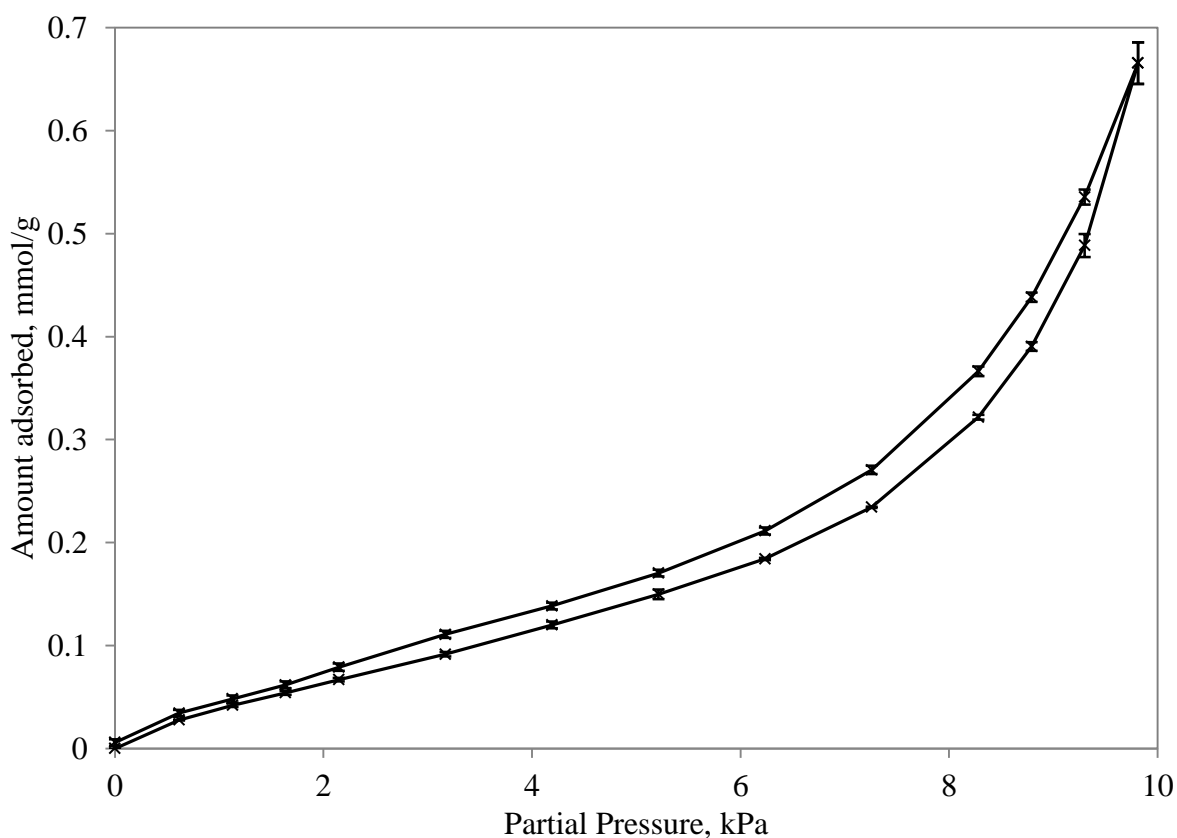


Figure 3. The average of three runs with error bars for a sorption isotherm of cyclohexane on a 2 g clay sample at 20°C.

Figure 3 shows good repeatability of equilibrium sorption data for a typical sample of cyclohexane adsorbed on clay. The upper line represent desorption and the lower line represents

adsorption. There are error bars present on the graph but many are too small to be seen. The lines joining the points are only present to indicate the trends in the results.

5.2 Classification of Isotherm

Figure 4 shows the typical shape of the equilibrium sorption isotherms for cyclohexane vapour adsorbed on a 50 mg clay sample at 20°C. The upper line of data is desorption and the lower line is adsorption showing that the shape of the isotherm is Type II with little hysteresis according to the isotherm classification by BDDT [23]. The same Type II classification of cyclohexane adsorption was made by Hsing and Wade on alumina [27]. The hysteresis between adsorption and desorption have been attributed to the filling of the pores for adsorption and the overcoming of surface energies at the constrictions within the porous network for desorption [28].

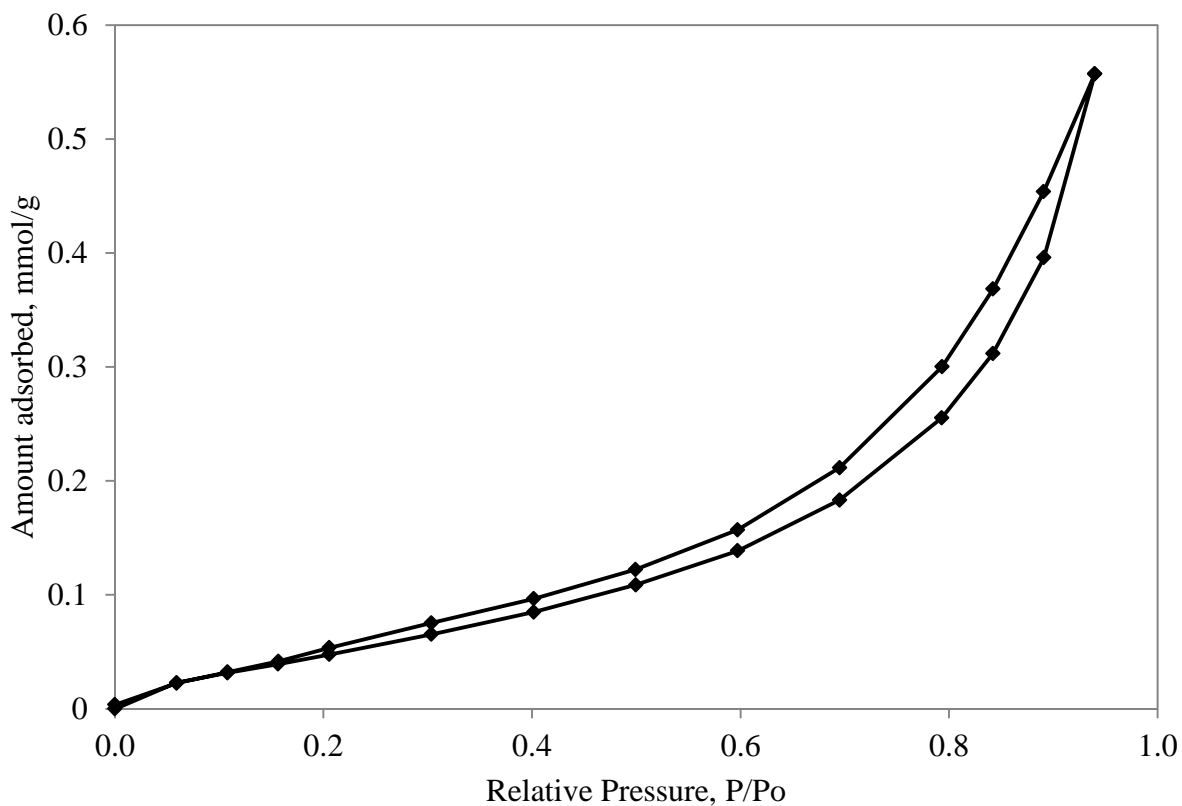


Figure 4. Sorption isotherm for cyclohexane on a 50 mg clay sample at 20°C.

5.3 Temperature Dependence of Isotherm

Figure 5 shows the effect of temperature on the amount of cyclohexane adsorbed. As expected, the amount of cyclohexane adsorbed decreases with increasing temperature. This effect is due to the nature of the adsorbate molecules. As the temperature increases, the molecules possess more kinetic energy and have a higher tendency toward the gas phase because the molecules begin to repel each other and are less likely to adsorb to the substrate. Also, the S-shape becomes less prominent with increasing temperature because multilayer adsorption is shifted to higher partial pressures as the temperature is increased. Essentially, the S-shape has simply shifted to the right, beyond the scale of the graph.

Typically, adsorption isotherms are plotted as amount adsorbed versus relative pressure, but for the purposes of this investigation, the plots are often amount adsorbed versus partial pressure. Plotting the data in this way makes it easier to see trends in the data and can be seen by comparing Figure 5 and Figure 6.

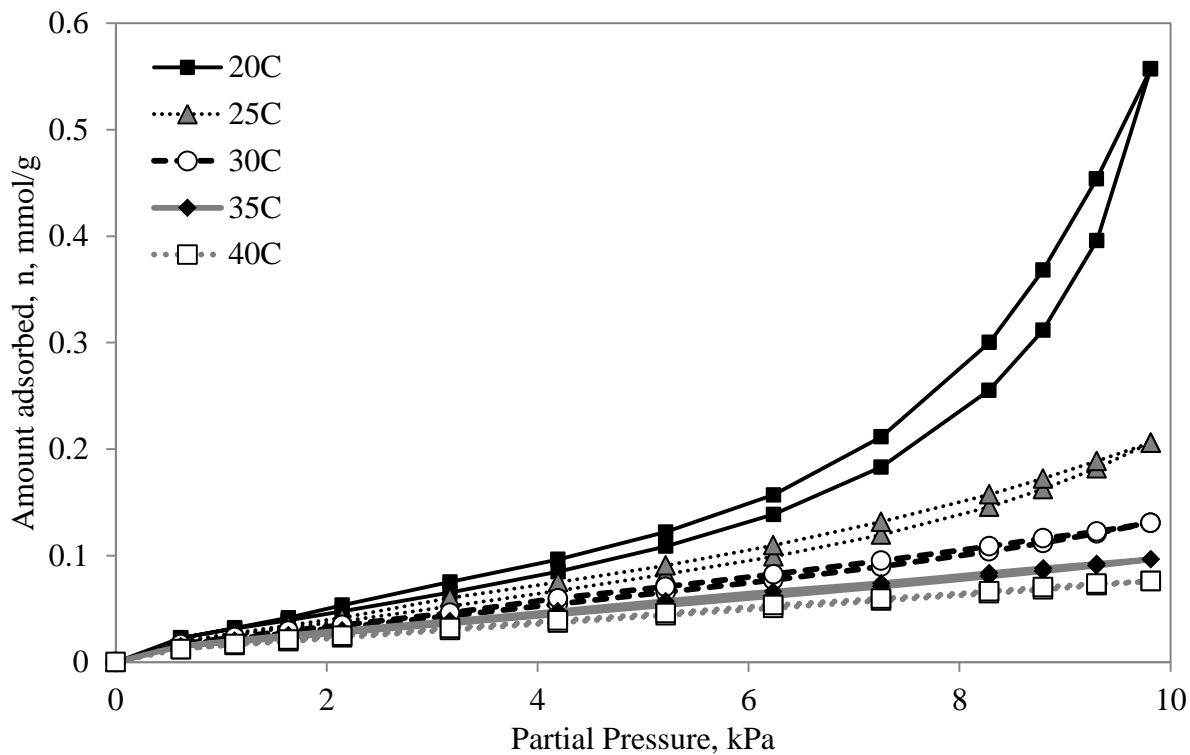


Figure 5. Sorption isotherms at three temperatures for cyclohexane on a 50 mg sample of clay.

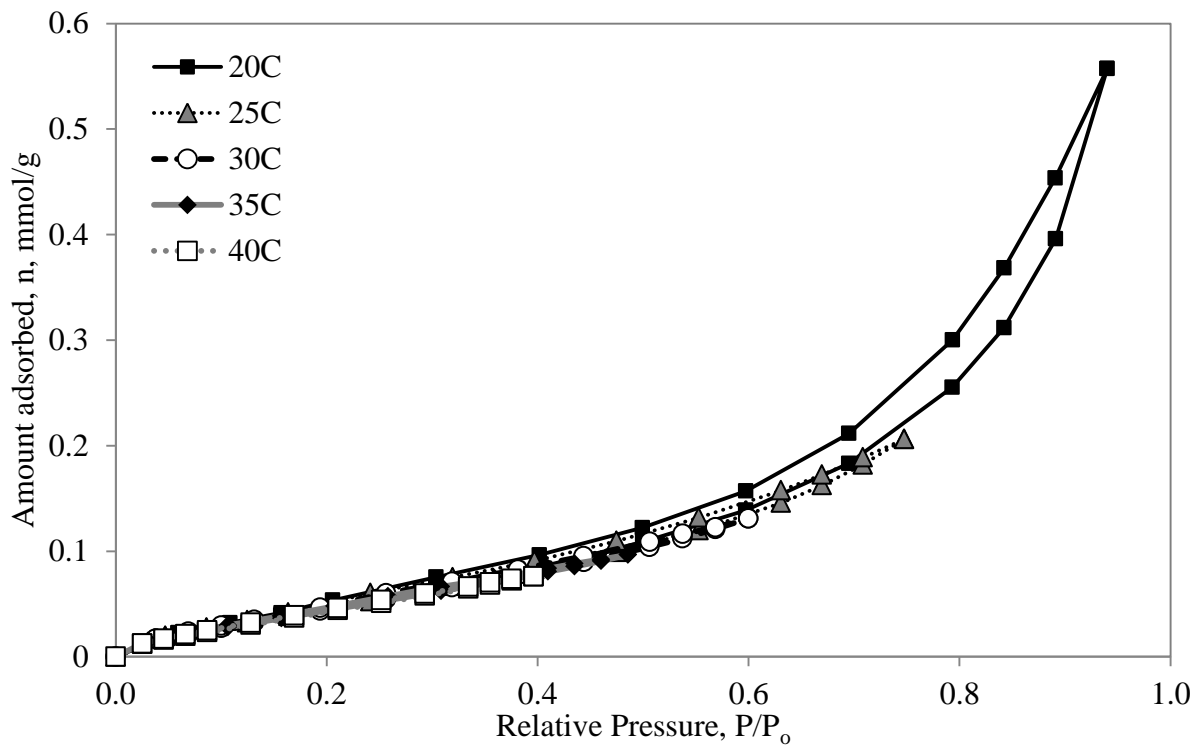


Figure 6. Classically plotted sorption isotherms at three temperatures for cyclohexane on a 50 mg sample of clay.

5.3.1 BET Monolayer Coverage

The BET monolayer for cyclohexane on clay at various temperatures is shown in Figure 7. The monolayer decreased slightly with increasing temperature. The BET plots using equation (1), although not shown here, were not linear. This phenomenon has also been noted by Hsing and Wade [27] and Gregg [25].

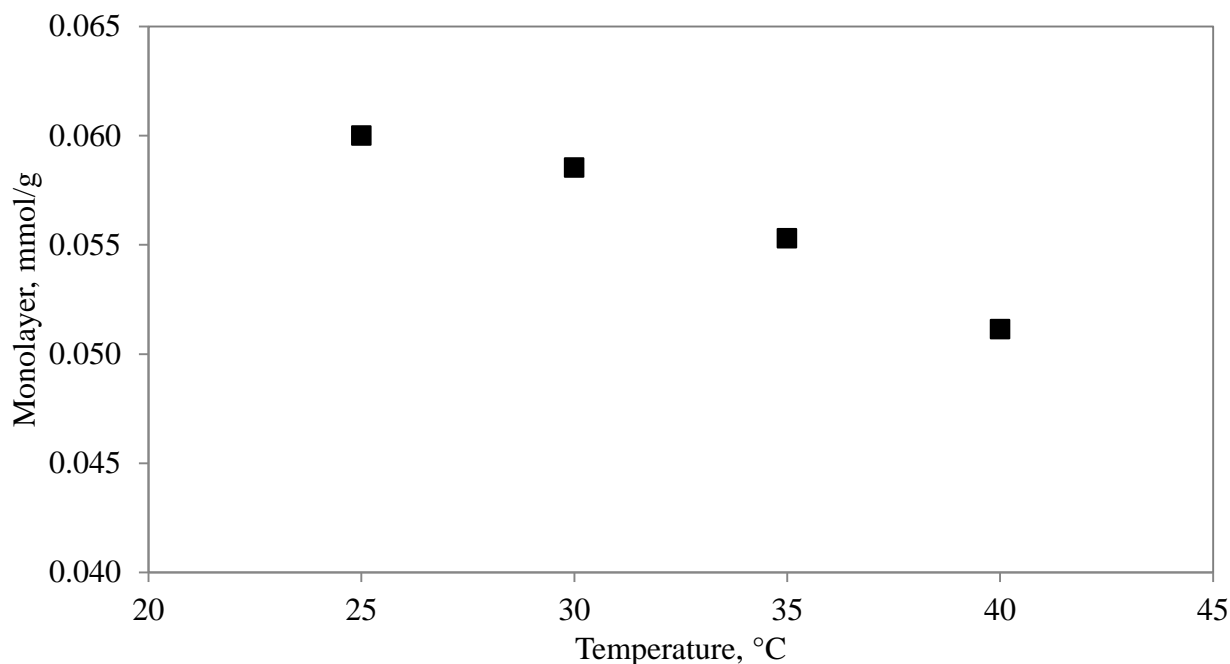


Figure 7. BET monolayer for cyclohexane on clay at several temperatures for a 50mg sample.

The average BET monolayer coverage for temperatures from 25°C to 40°C is 0.056 mmol/g for a 50 mg sample. Given that the area of a single cyclohexane molecule is 0.417 nm² [29] then the area covered by cyclohexane is calculated to be 14.1 m²/g. For an average surface area of kaolinite of 21.4 m²/g [30], this results in a 65.7 % coverage of the surface at the monolayer. The aggregation of clay, differences between the oil sands fines and pure kaolinite, and the heterogeneity of the surface sites could contribute to a reduction in the monolayer coverage of the substrate.

Table 4. Monolayer coverage for toluene and cyclohexane on centrifuged solids, and 2000 mg samples of kaolinite and clay at 30°C.

Adsorbent	Adsorbate	Monolayer (mmol/ g solids)
Centrifuged solids	Toluene	0.069*
Kaolinite	Toluene	0.109*
Clay	Cyclohexane	0.081
Kaolinite	Cyclohexane	0.083

*Obtained from unpublished work by Xiaoli Tan

To gain some perspective, the monolayer of cyclohexane on clay in this investigation is compared to values obtained from previous work and are shown in Table 4. Literature values for the monolayer of cyclohexane on clay or kaolinite were not obtainable. Toluene provides a good comparison due to its similar size and polarity. Centrifuged solids are fine solids, less than 45 μm , that were obtained during the non aqueous extraction process in a related study. The table shows that the values obtained in this investigation for the monolayer of cyclohexane on clay are reasonable in comparison with results from previous work.

5.3.2 Enthalpy of Adsorption

The absolute value of enthalpies of adsorption and desorption for cyclohexane on clay were calculated using the Van't Hoff Isochore equation (7) and are shown in Figure 8. The enthalpies of adsorption for the range of 0.03 to 0.05 mmol/g of adsorbed cyclohexane indicate a trend of decreasing value with increasing amount adsorbed. However, the enthalpies of desorption show no clear trend with amount adsorbed. In this investigation, the average enthalpy of adsorption of cyclohexane on clay was found to be about 40 kJ/mol which is reasonable in comparison to the only literature value comparable of 53.6 kJ/mol for cyclohexane adsorbed on kaolinite at 150°C [31]. Enthalpies of adsorption can also be calculated from the BET equation, however the value obtained is calculated from one temperature, can vary greatly, and also depends on the fractional coverage of the substrate at the monolayer [25].

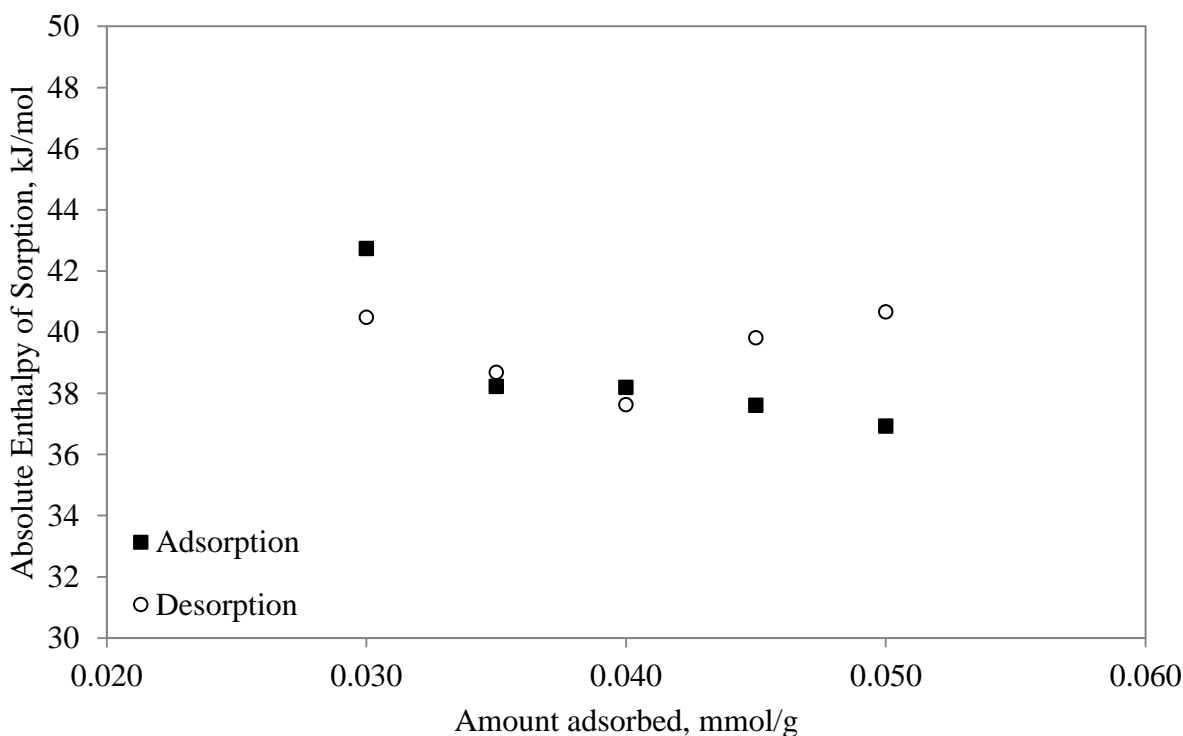


Figure 8. Absolute value of enthalpies of sorption for adsorption and desorption of cyclohexane on clay.

5.4 Kinetics of Adsorption and Desorption

5.4.1 Repeatability of Adsorption and Desorption

Figure 9 shows that repeatability was much better for the desorption phase than for the adsorption phase. The rate constants were calculated based on the linear driving force model which is explained in the chapter on theory. Some variation in rate constant was expected, however the low level of variation in the desorption phase indicates that diffusive resistance may be the limiting factor for desorption. The desorption rate constants are lower than the adsorption rate constants. This means that desorption is slower than adsorption.

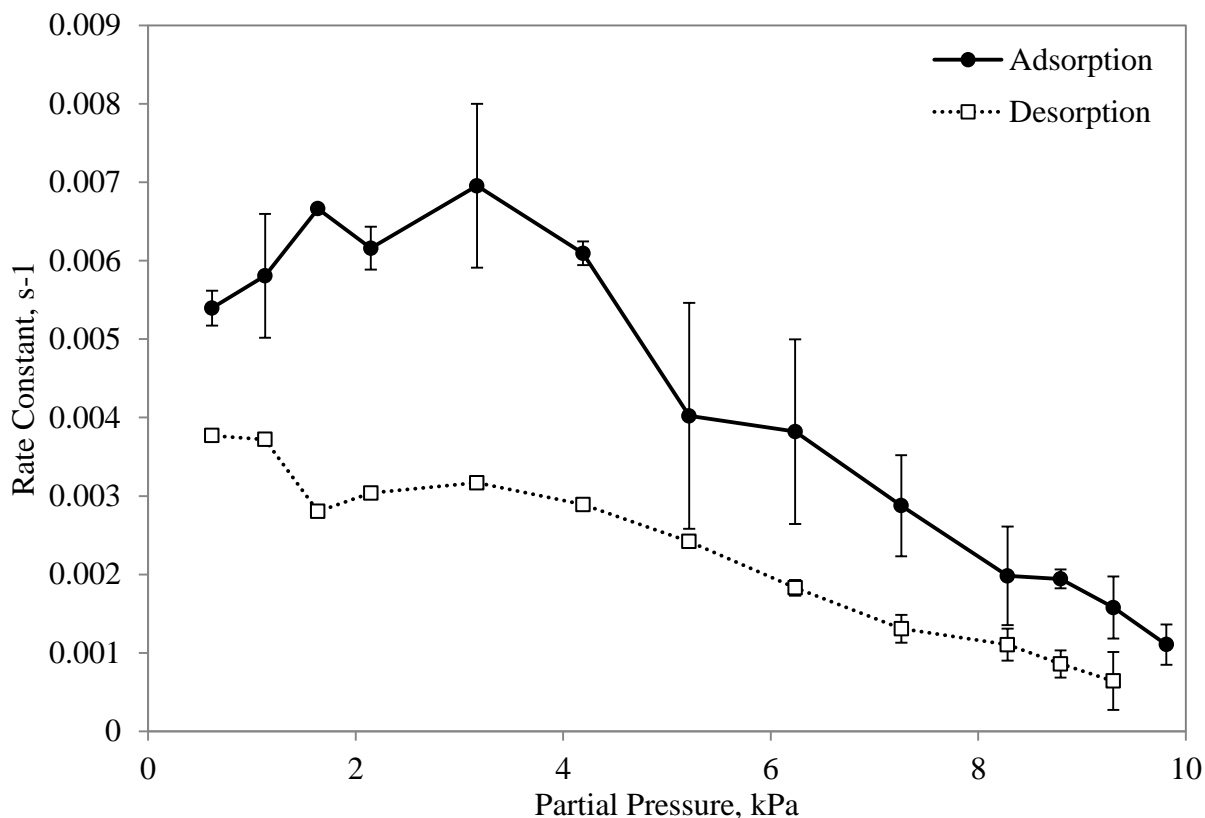


Figure 9. Sorption kinetics for three runs of cyclohexane on a 2 g clay sample at 20°C.

5.4.2 The Effect of Temperature on Sorption Kinetics

Kinetic rate constants can be defined as the reciprocal of time to equilibrium. Therefore, as kinetic rate increases, time to equilibrium decreases and the reaction or process speeds up. Figure 10 to Figure 16 show the effect of temperature, amount of cyclohexane adsorbed, and solvent concentration partial pressure on the kinetic rate constants of cyclohexane on a 50 mg sample of clay. Figure 10 and Figure 11 show kinetic rate constants as a function of partial pressure, while Figure 12 and Figure 13 as a function of amount adsorbed. By plotting rate constants versus amount adsorbed, one can more easily visualize how the molecules are interacting on the surface. The peaks in Figure 12 between 0.02 and 0.04 mmol/g seem to be related to the monolayer coverage of the substrate. At all temperatures, these peaks occur before the monolayer is reached, which suggests that as the substrate is covered the solvent-solid interaction is weakened. During the desorption phase shown in Figure 13, the rate constants rapidly increase around 0.05 mmol/g as the amount adsorbed decreases and peak between 0.01 and 0.03 mmol/g (moving

along the graph from right to left). This suggests that below the monolayer coverage, desorption rates are increased. This effect shows promise for the solvent recovery process and an opportunity for optimization.

The three dimensional representation in Figure 14 simultaneously shows the effects of partial pressure and temperature on the rate constants and Figure 15 simultaneously shows the effects of partial pressure and temperature on the amount adsorbed. Figure 16 shows the effects of partial pressure and amount adsorbed on the rate constants. In order to visualize a trend, data points were connected by lines to form a surface. All three figures are for the adsorption phase only.

A clear trend can be seen in the adsorption phase: the kinetic rate rapidly increases with solvent concentration and amount adsorbed, reaches a maximum value then slowly decreases. This suggests strongly that cyclohexane is more attracted to itself than the clay substrate and the interaction between cyclohexane and the clay is weak. This was also observed by Hsing and Wade between cyclohexane and alumina [27]. Due to the high frequency of exposed Al atoms on a typical kaolinite clay, it may be considered comparable to alumina as a substrate. As expected, kinetic rate constants tended to increase with temperature for obvious reasons. Trends in the adsorption phase tended to be more prominent than in the desorption phase.

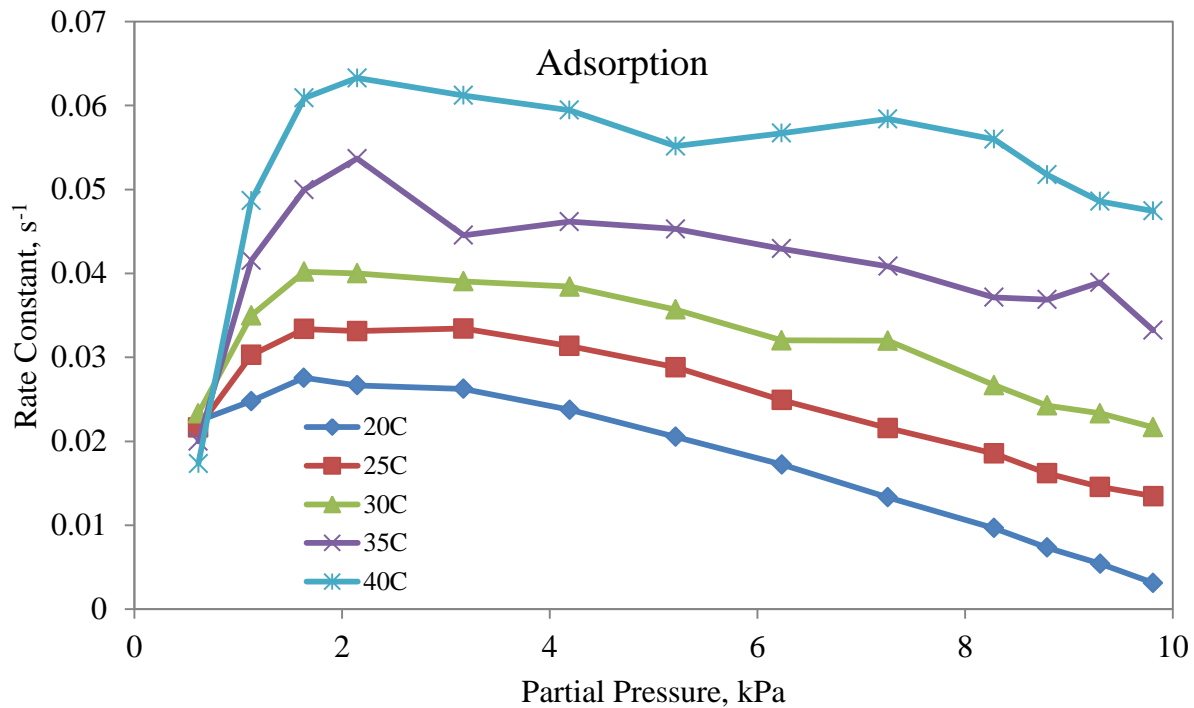


Figure 10. Adsorption rate constants for cyclohexane on a 50 mg clay sample at various temperatures.

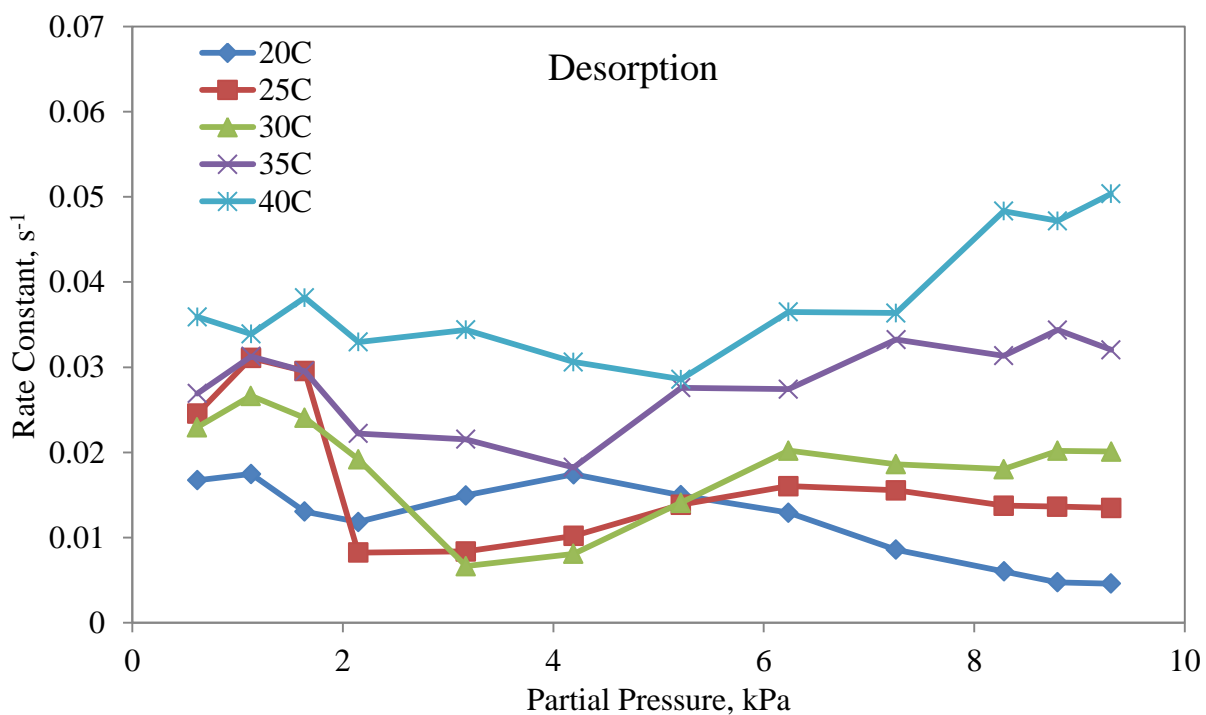


Figure 11. Desorption rate constants for cyclohexane on a 50 mg clay sample at various temperatures.

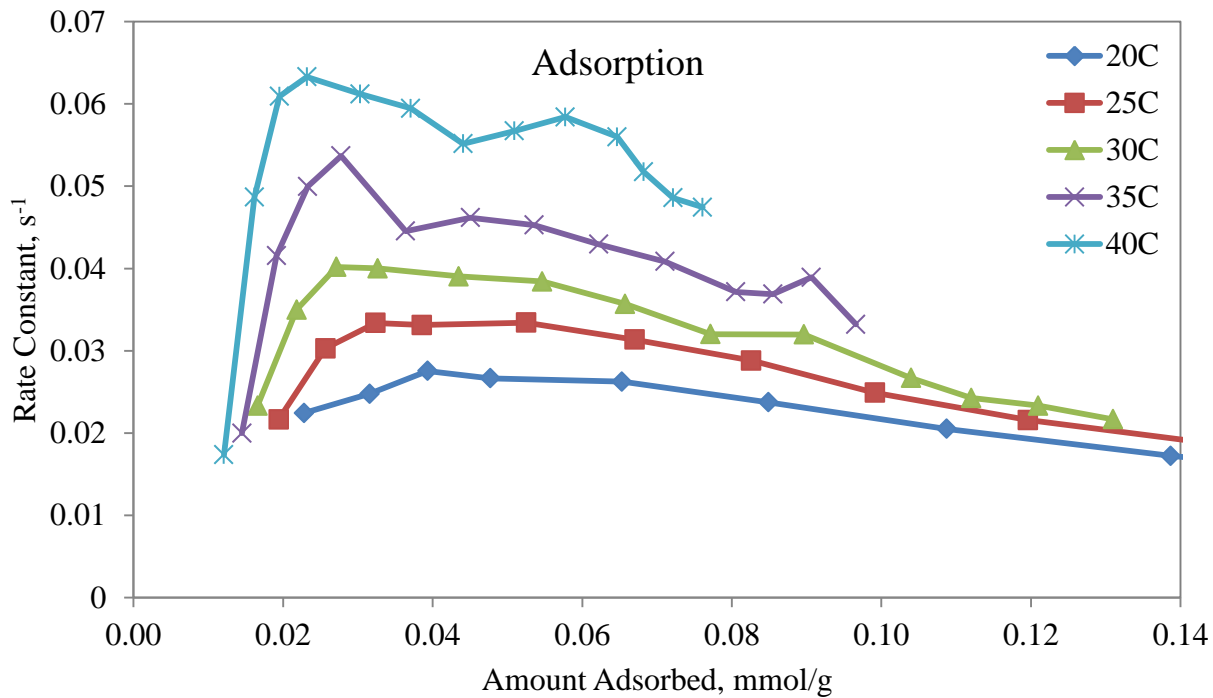


Figure 12. Adsorption rate constants versus amount of cyclohexane adsorbed on a 50 mg clay sample at various temperatures.

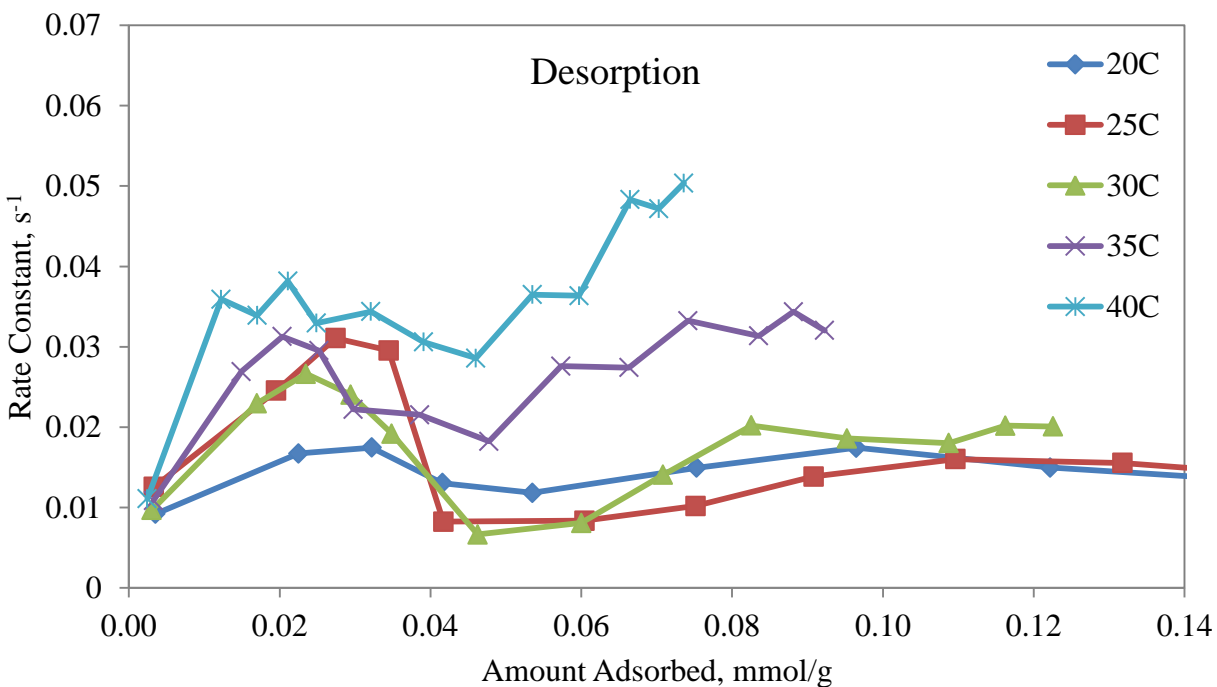


Figure 13. Desorption rate constants versus amount of cyclohexane adsorbed on a 50 mg clay sample at various temperatures.

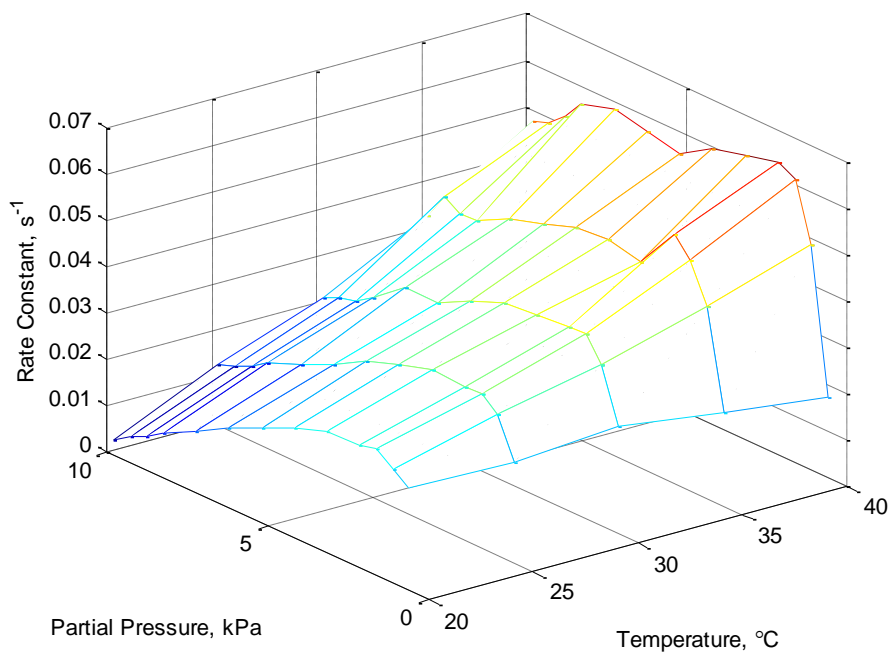


Figure 14. Three dimensional graph of rate constant versus partial pressure versus temperature of cyclohexane adsorbed on a 50 mg sample of clay.

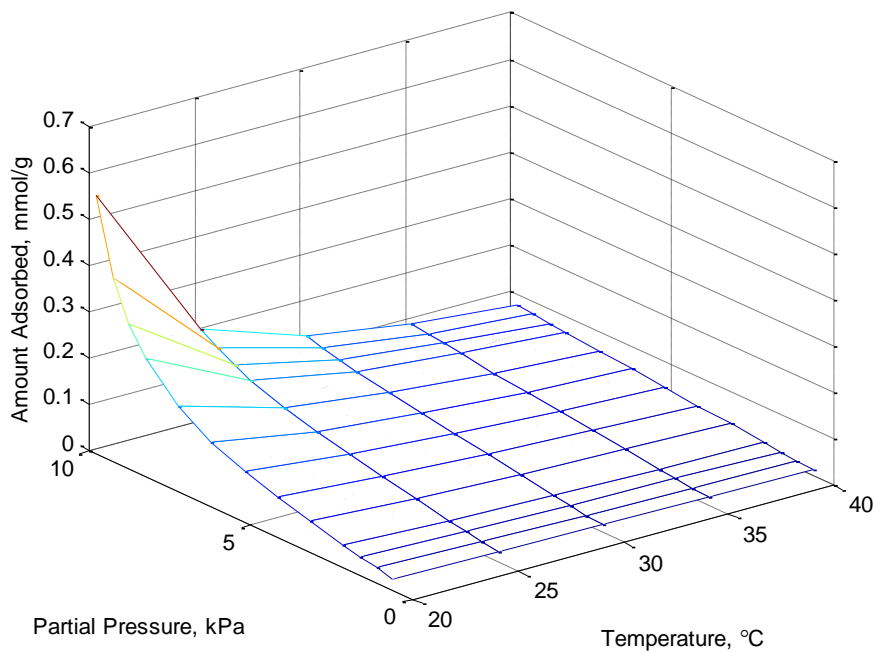


Figure 15. Three dimensional graph of amount adsorbed versus partial pressure versus temperature of cyclohexane adsorbed on a 50 mg sample of clay.

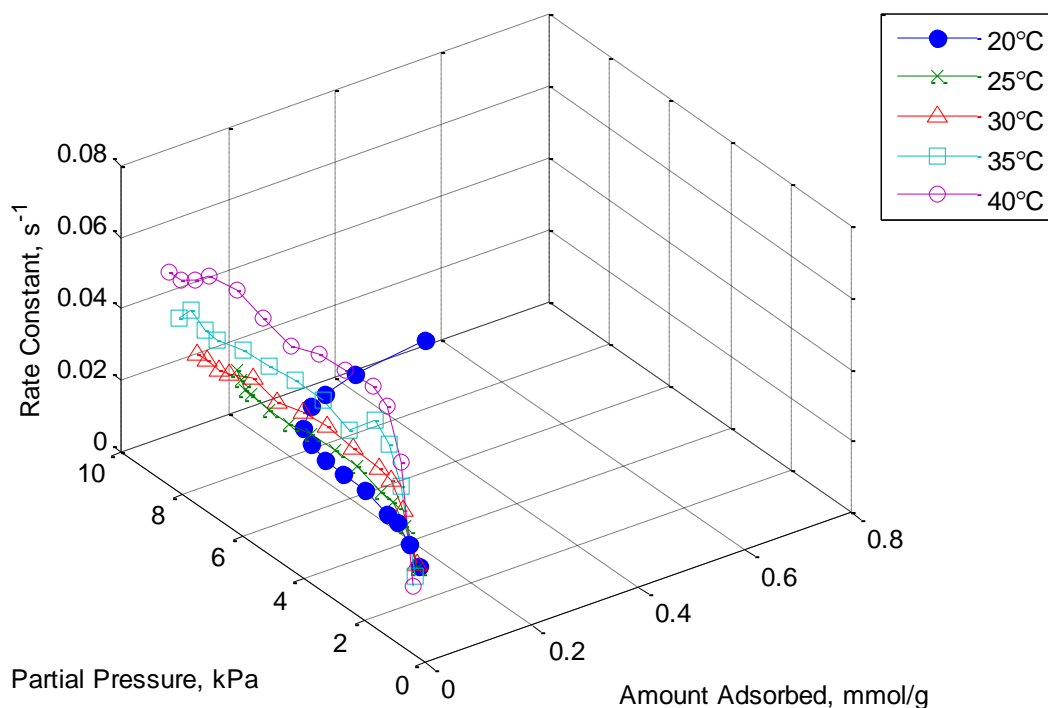


Figure 16. Three dimensional graph of rate constant versus partial pressure versus amount adsorbed at various temperatures for cyclohexane adsorbed on a 50 mg sample of clay.

5.5 Effect of Sample Size and Sampling

5.5.1 Equilibrium Sorption

Figure 17 shows that there is no effect on equilibrium sorption amount due to sample size. The 150 mg and 800 mg samples were produced by sub-sampling from the 2000 mg sample. This produced nearly identical equilibrium sorption isotherms. The difference for the 50 mg sample can be attributed to sample error caused by sampling too small from a very heterogeneous mixture. Repeatability of results by others is nearly impossible due to the heterogeneity of the clay because it is sampled from a real oil sand ore.

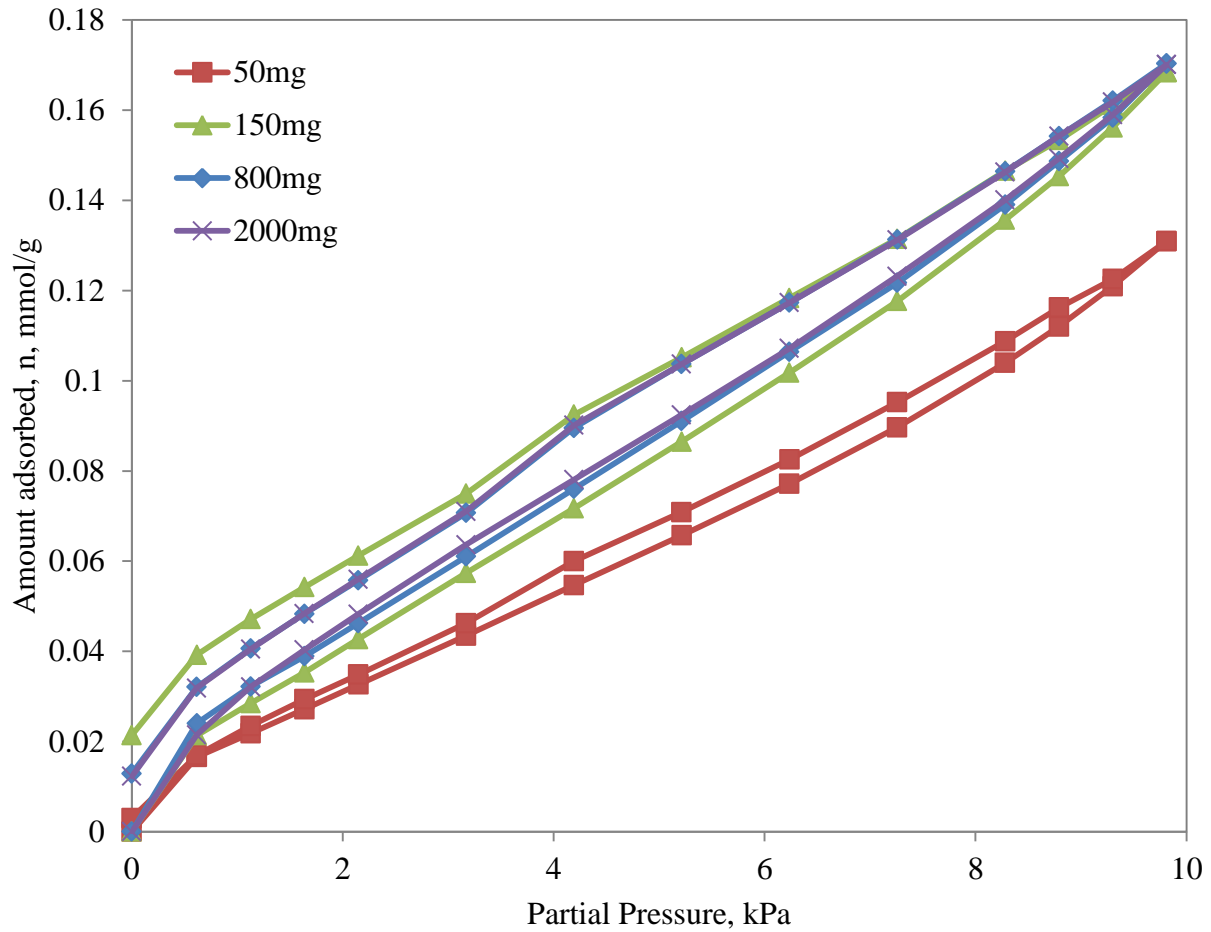


Figure 17. The effect of sample size on equilibrium sorption of cyclohexane on clay at 30°C.

5.5.2 Sorption Kinetics

Figure 18 to Figure 22 show the effect of sample size on the kinetic rate constants of cyclohexane sorption behaviour on clay at 30°C. Figure 20 shows the clearest trend that, as expected, the kinetic rate constants decrease with increasing sample size. This supports the theory of the effect of increasing bulk diffusion. As the sample size increases, the molecules have further to travel in order to reach equilibrium. Again, trends with the desorption data were less clear.

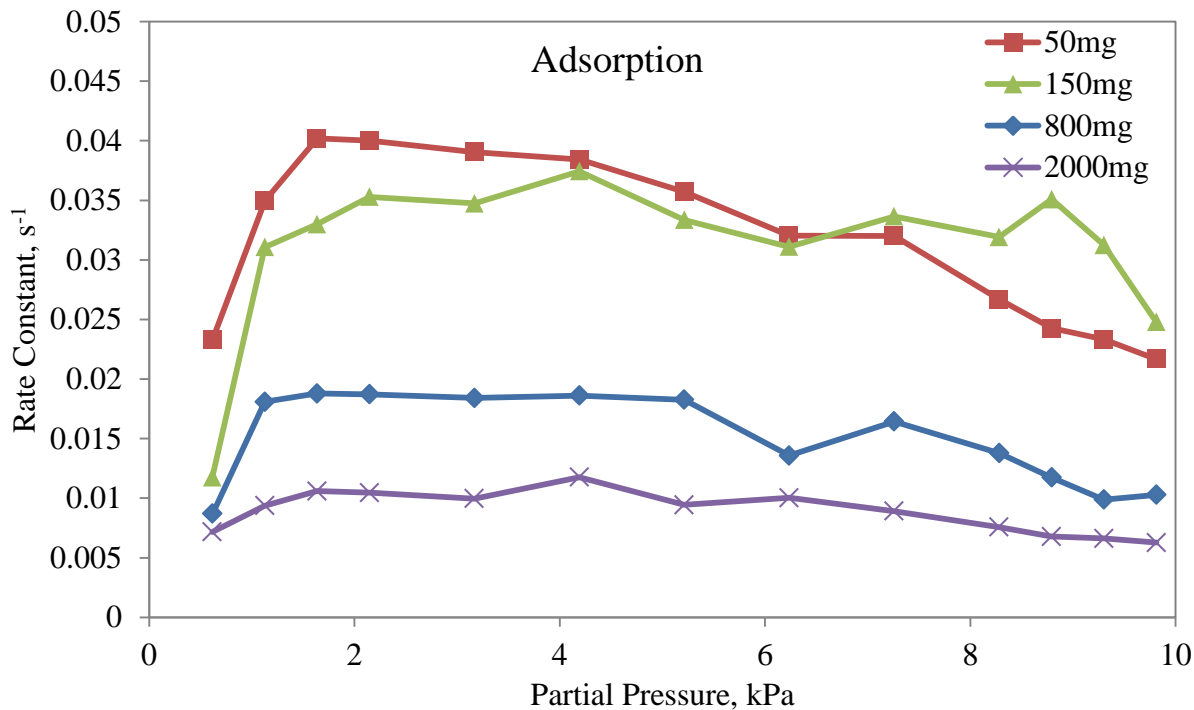


Figure 18. Adsorption rate constants for cyclohexane on clay at 30°C for various sample sizes.

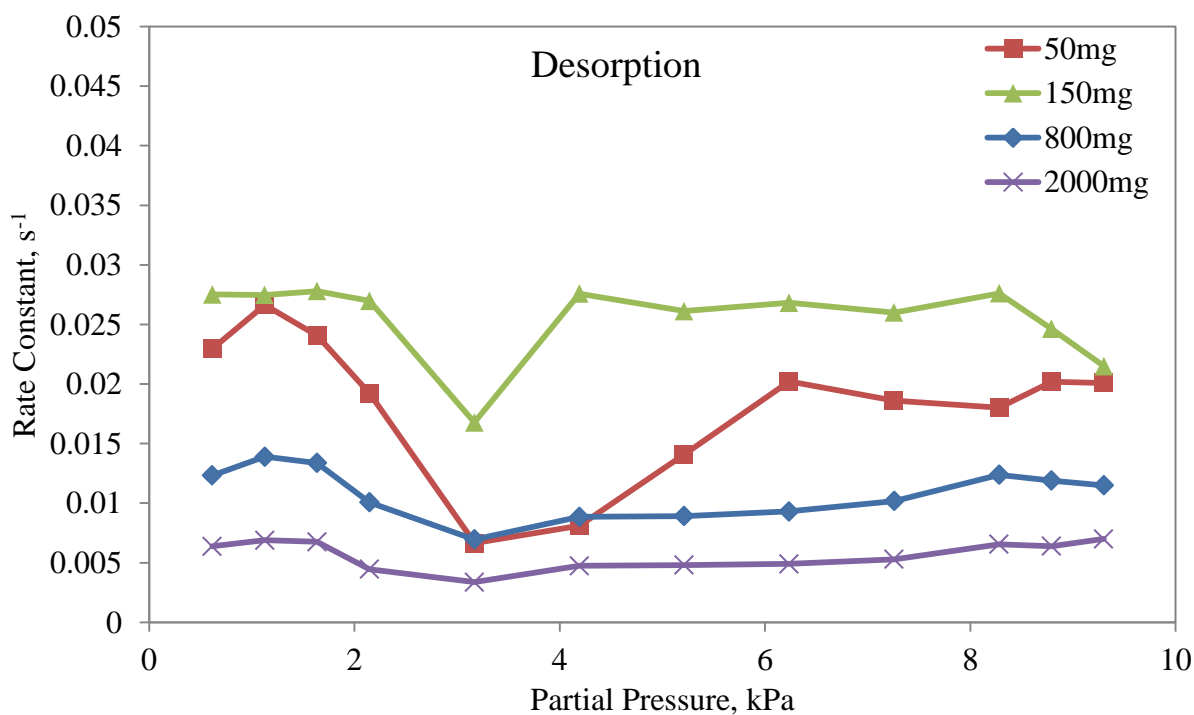


Figure 19. Desorption rate constants for cyclohexane on clay at 30°C for various sample sizes.

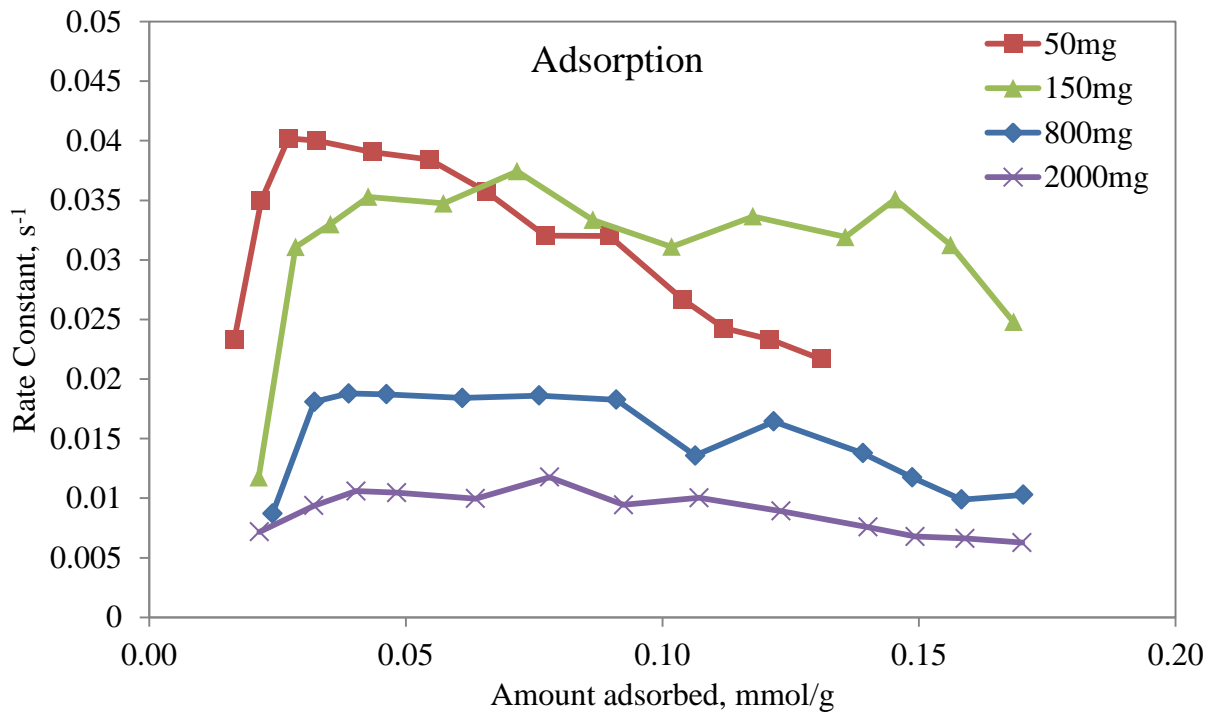


Figure 20. Adsorption rate constants versus amount of cyclohexane adsorbed on clay at 30°C for various sample sizes.

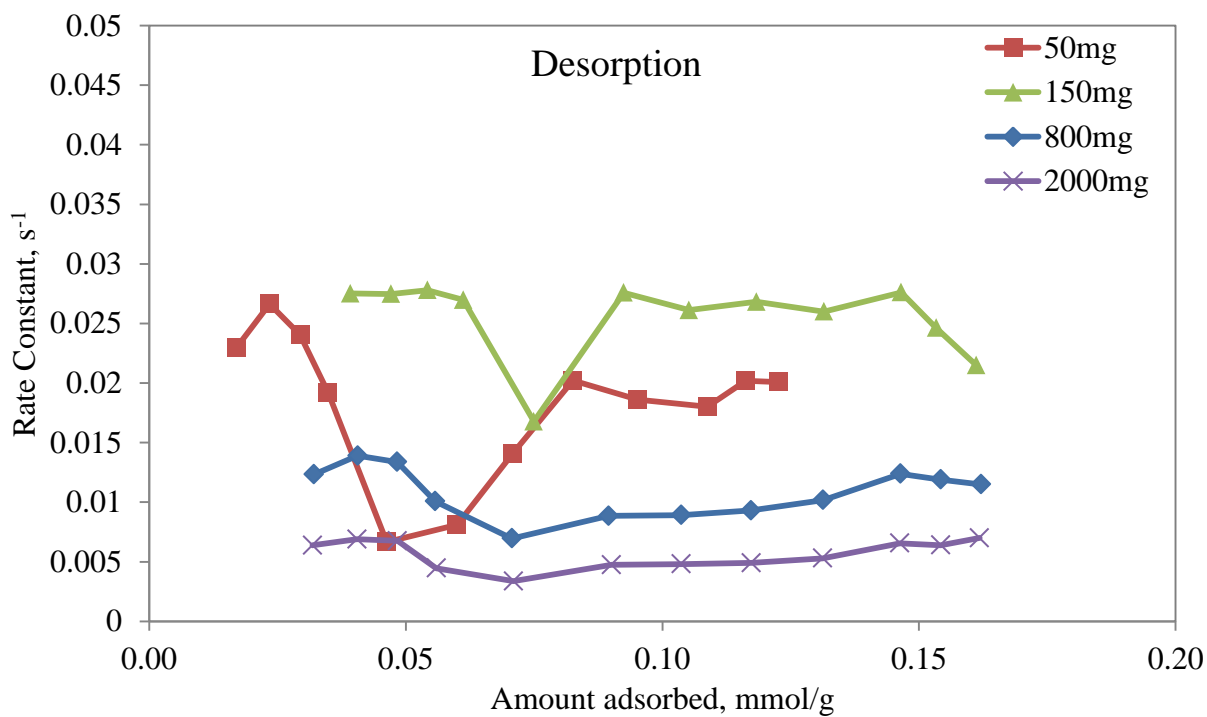


Figure 21. Desorption rate constants versus amount of cyclohexane adsorbed on clay at 30°C for various sample sizes.

The mean kinetic rate constants at 30°C as a function of dry sample size are shown in Figure 22. These average values were calculated from the plateau-like regions in Figure 18 from 2 to 4 kPa and Figure 19 from 6 to 8 kPa. The error bars indicate the variance in the plateau rather than multiple experiments. This enables the visualization of a trend that the kinetic rate constants increase with decreasing sample size. Mean rate constants for adsorption were always greater than those for desorption for the same sample size. This effect suggests that a limiting rate factor exists, such as a diffusion. The small decrease in mean desorption kinetic rate from the 150 mg sample to the 50 mg sample needs more experiments to confirm this trend.

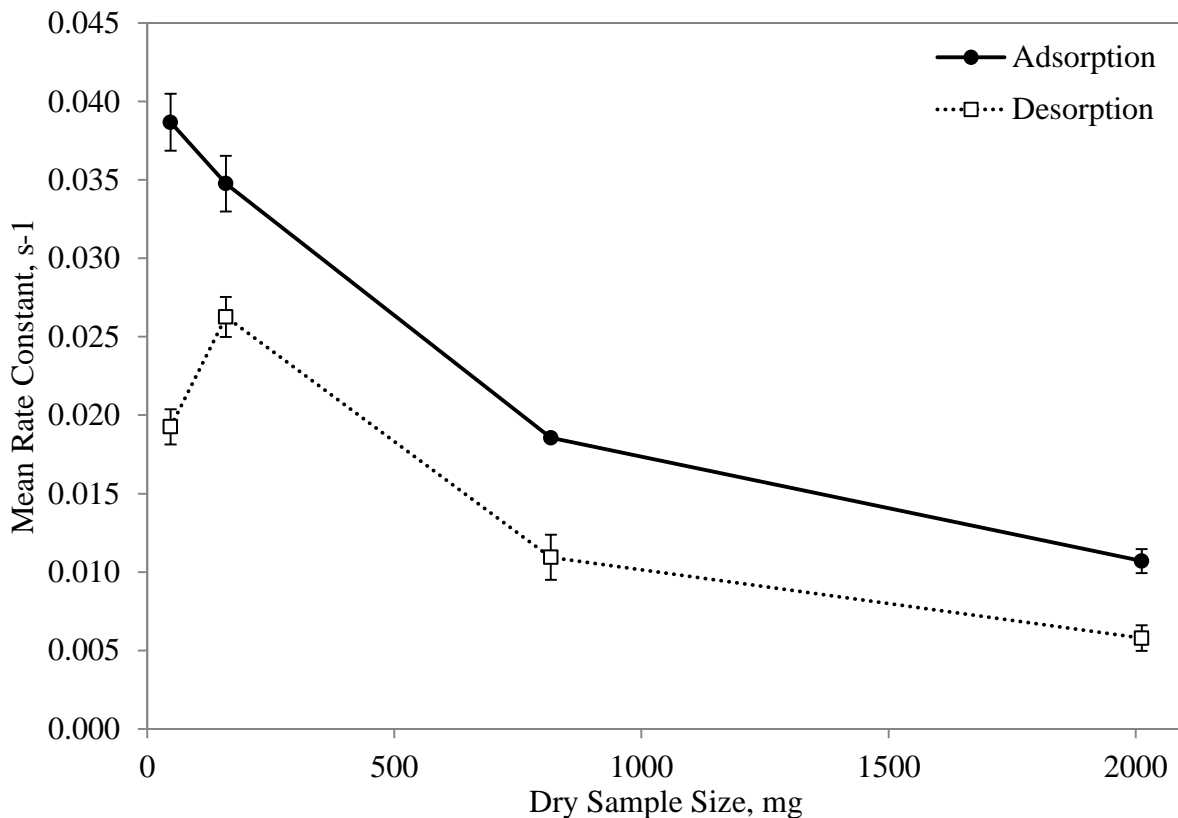


Figure 22. Mean rate constants versus sample size for adsorption and desorption of cyclohexane on clay at 30°C.

It was desired to test larger sample sizes until the kinetic rate constants showed signs of levelling off in order to show the effect of increasing bulk diffusion. Unfortunately, the maximum capacity of the sample bucket was reached with the 2 g clay sample. If smaller sample sizes were tested, the rate constants for adsorption and desorption would become equal.

6.0 Conclusions

The adsorptive behaviour of cyclohexane vapour on clay from oil sands was characterized. The factors of temperatures between 20°C and 40°C, sample sizes from 50 mg to 2000 mg, and partial pressures from 0 to 9.3 kPa and their effect on amount adsorbed and sorption kinetics were explored. The characterization provides data for future modelling and process design.

The isotherm for cyclohexane on clay was classified as a Type II isotherm according to BDDT classification. The amount of cyclohexane adsorbed was found to be up to 0.67 mmol/g when equilibrated at 9.8 kPa partial pressure at 20°C. Increasing temperature resulted in decreasing adsorbed amount of cyclohexane. There was minimal effect on adsorbed amount when the sample size was changed, as long as it was sampled correctly.

The BET monolayer coverage varied with temperature. For the range of 20°C to 40°C, the average BET monolayer coverage was calculated to be 0.056 mmol/g for a 50 mg sample. The BET monolayer coverage was calculated to be 0.081 mmol/g for the 2000 mg sample of clay at 30°C, which is comparable to the 0.083 mmol/g monolayer coverage of a sample of pure kaolinite of the same size at the same temperature.

The enthalpies of adsorption and desorption varied with the amount adsorbed and ranged from 36.9 to 42.7 kJ/mol for adsorption and 37.6 to 40.7 kJ/mol for desorption at the range of temperatures explored in this study. The average enthalpy of adsorption and desorption was calculated to be about 40 kJ/mol which is similar to the literature value for cyclohexane on kaolinite.

For a 50 mg sample, kinetic rate constants were found in the range of 0.003 to 0.063 s⁻¹ for adsorption and 0.005 to 0.050 s⁻¹ for desorption. Increasing temperature tended to result in increasing rate constants while increasing sample size decreased rate constants. Mean kinetic rate constants ranged from 0.011 to 0.039 s⁻¹ for adsorption and 0.006 to 0.026 s⁻¹ for desorption. Increasing sample size resulted in decreasing mean kinetic rate constants in general.

References

- [1] Y. Jin, W. Liu, Q. Liu and A. Yeung, "Aggregation of silica particles in non-aqueous media," *Fuel*, vol. 90, pp. 2592-2597, 2011.
- [2] H. A. W. Kaminsky, T. H. Etsell, D. G. Ivey and O. Omotoso, "Distribution of clay minerals in the process streams produced by the extraction of bitumen from Athabasca oil sands," *Canadian Journal of Chemical Engineering*, Vols. 87-93, p. 85, 2009.
- [3] F. W. Camp, "Processing athabasca tar sands - tailings disposal," *Canadian Journal of Chemical Engineering*, vol. 55, pp. 581-591, 1977.
- [4] H. Leung and C. R. Phillips, "Solvent extraction of mined Athabasca oil sands," *Ind. Eng. Chem. Fundam.*, vol. 24, pp. 373-379, 1985.
- [5] H. Nikakhtari, L. Vagi, P. Choi, Q. Liu and M. Gray, "Solvent Screening for Non-Aqueous Extraction of Alberta Oil Sands (accepted for publication)," *Canadian Journal of Chemical Engineering*.
- [6] A. Hooshar, P. Uhlik, Q. Liu, T. H. Etsell and D. G. Ivey, "Clay minerals in nonaqueous extraction of bitumen from Alberta oil sands Part 1. Nonaqueous extraction procedure," *Fuel Processing Technologies*, vol. 94, pp. 80-85, 2012.
- [7] Heritage Community Foundation, "Alberta Inventors and Inventions - Karl Clark," [Online]. Available: http://web.archive.org/web/20060305194624/http://www.abheritage.ca/abinvents/inventors/karlclark_biography.htm. [Accessed 12 July 2012].
- [8] F. H. Poettmann and e. al., "Use of a soluble oil in the extraction of hydrocarbons from oil sands". US Patent 3392105, 9 July 1968.
- [9] J. Y. Low, "Hydrotreating supercritical solvent extracts in the presence of alkane extractants". US Patent 4397736, 22 April 1986.

- [10] A. Hooshiar, P. Uhlik, O. B. Adeyinka, Q. Liu, T. H. Etsell and D. G. Ivey, "Extraction of bitumen from Alberta oil sands using mixtures of toluene and heptane," *Fuel*, 2010.
- [11] T. A. Pittman and J. L. Woods, "Bitumen extraction apparatus including endless perforate conveyor and plural solvent-spray means". US Patent 3856474, 24 Dec. 1974.
- [12] B. D. Sparks and F. W. Meadus, "Solvent extraction spherical agglomeration of oil sands". Ottawa, Canada Patent 4719008, 12 Jan. 1988.
- [13] B. D. Sparks and F. W. Meadus, "A combined solvent extraction and agglomeration technique for the recovery of bitumen from tar sands," *Energy Processing/Canada*, pp. 55-61, 1979.
- [14] M. Subramanian and F. V. Hanson, "Supercritical fluid extraction of bitumens from Utah oil sands," *Fuel Processing Technology*, vol. 55, no. 1, pp. 35-53, 1998.
- [15] K. Haugen, O. Kvernfold, A. Ronold and R. Sandberg, "Sand erosion of wear-resistant materials: Erosion in choke valves," *8th International Conference on Erosion by Liquid and Solid Impact*, Vols. 186-187, no. 1, pp. 179-188, 1995.
- [16] R. Raghavan, E. Coles and D. Dietz, "Cleaning excavated soil using extraction agents: a state-of-the-art review," *Journal of Hazardous Materials*, vol. 26, pp. 81-87, 1991.
- [17] K. T. Valsarj and L. J. Thibodeaux, "Equilibrium adsorption of chemical vapors on surface soils, landfills and landfarms - a review," *Journal of Hazardous Materials*, vol. 19, pp. 79-99, 1988.
- [18] Y.-H. Shih and S.-C. Wu, "Distinctive sorption mechanisms of soil organic matter and mineral components as elucidated by organic vapor uptake kinetics," *Environmental Toxicology and Chemistry*, vol. 24, no. 11, pp. 2827-2832, 2005.
- [19] I. Jarraya, S. Fourmentin, M. Benzina and S. Bouaziz, "VOC adsorption on raw and modified clay materials," *Chemical Geology*, vol. 275, no. 1-2, pp. 1-8, 2010.
- [20] H. Chon and D. H. Park, "Diffusion of cyclohexanes in ZSM-5 zeolites," *Journal of Catalysis*, vol. 114, pp. 1-7, 1988.

- [21] A. J. Fletcher and K. M. Thomas, "Adsorption and desorption kinetics of n-octane and n-nonane vapors on activated carbon," *Langmuir*, vol. 15, pp. 6909-6914, 1999.
- [22] M.-H. Lai, R. Q. Chu, H.-C. Huang, S.-H. Shu and T.-W. Chung, "Equilibrium isotherms of volatile alkanes, alkenes, and ketones on activated carbon," *Journal of Chemical Engineering Data*, vol. 54, pp. 2208-2215, 2009.
- [23] S. Brunauer, L. S. Deming, W. S. Deming and E. Teller, *J. Amer. Chem. Soc.*, vol. 62, p. 1723, 1940.
- [24] I. Langmuir, *J. Amer. Chem. Soc.*, vol. 38, p. 2221, 1916.
- [25] S. J. Gregg, *Adsorption Surface Area and Porosity*, 2nd ed., London: Academic Press, 1982, pp. 44, 53.
- [26] S. Brunauer, P. H. Emmett and E. J. Teller, *J. Am. Chem. Soc.*, vol. 60, p. 309, 1938.
- [27] H. Hsing and W. Wade, "Weak interaction of Cyclohexane with alumina," *J. Coll. Int. Sci.*, vol. 47, pp. 271-588, 1974.
- [28] W. M. C. Conner, "Analyses of (ad)-sorption for the estimation of pore-network dimensions and structure," *Journal of Porous Materials* 2, pp. 191-199, 1996.
- [29] A. L. McClellan and H. F. Harnsberger, "Cross-sectional areas of molecules adsorbed on solid surfaces," *Journal of Colloid and Interface Science*, vol. 23, pp. 577-599, 1967.
- [30] L. A. G. Aylmore, "Gas sorption in clay mineral systems," *Clays and Clay Minerals*, vol. 22, pp. 175-183, 1974.
- [31] S. Hwang and M. Blanco, *J. Phys. Chem. B*, vol. 105, p. 4124, 2001.
- [32] R. Humayun and D. Tomasko, "High-resolution adsorption isotherms of supercritical carbon dioxide on activated carbon," *AIChE Journal*, vol. 46, no. 10, p. 2065, 2000.
- [33] S. Sircar and J. R. Hufton, "Why does the linear driving force model for adsorption kinetics work?," *Adsorption*, vol. 6, p. 137, 2000.
- [34] D. E. Cormack, J. M. Kenchington, C. R. Phillips and P. J. Leblanc, "Parameters and

mechanisms in the solvent extraction of mined athabasca oil sand," *Canadian Journal of Chemical Engineering*, vol. 55, pp. 572-580, 1977.

- [35] T. L. Gibson, A. S. Abdul, W. A. Glasson, C. C. Ang and D. W. Gatlin, "Vapor extraction of volatile organic compounds from clay soil: a long-term field pilot study," *Ground Water*, vol. 31, no. 4, pp. 616-626, 1993.
- [36] G. Anitescu and L. L. Tavlarides, "Supercritical extraction of contaminants from soils and sediments," *Journal of Supercritical Fluids*, vol. 38, pp. 167-180, 2006.
- [37] O. M. Ogunsola and N. Berkowitz, "Removal of heterocyclic S and N from oil precursors by supercritical water," *Fuel*, vol. 74, no. 10, pp. 1485-1490, 1995.
- [38] N. Berkowitz and J. Calderon, "Extraction of oil sand bitumens with supercritical water," *Fuel Processing Technology*, vol. 25, no. 1, pp. 33-44, 1990.